AD-A091 521 HUGHES RESEARCH LABS MALIBU CA F/G 20/6
INFRARED FIBER OPTICS.(U)
SEP 80 J A HARRINGTON, R R TURK F19628-78-C-0109
UNCLASSIFIED RADC-TR-80-290 NL

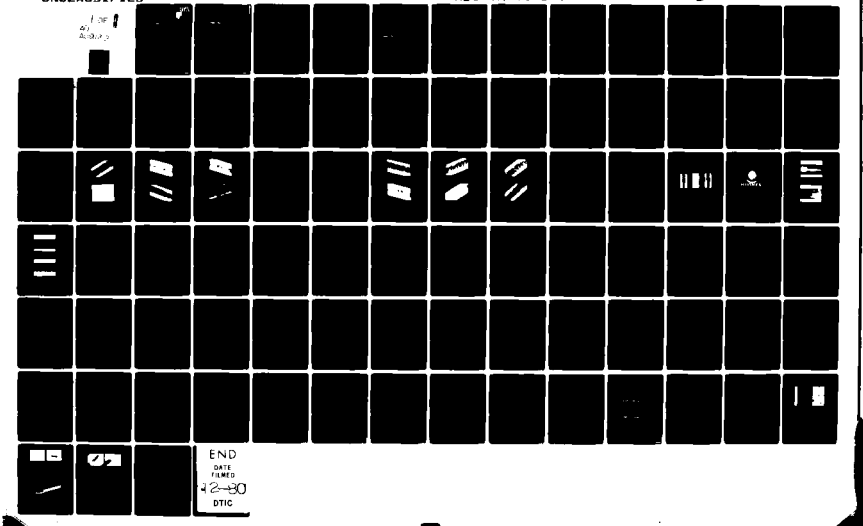

END
DATE FILMED
12-80
DTIC

RADC-TR-80-290
Final Technical Report
September 1980

INFRARED FIBER OPTICS

Hughes Research Laboratories

J. A. Harrington
D. M. Henderson
A. Standlee
R. R. Turk

ROME AIR DEVELOPMENT CENTER
Air Force Systems Command
Griffiss Air Force Base, New York 13441

This report has been reviewed by the RADC Public Affairs Office (PA) and is releasable to the National Technical Information Service (NTIS). At NTIS it will be releasable to the general public, including foreign nations.

RADC-TR-80-290 has been reviewed and is approved for publication.

APPROVED: Mark J. Hyc

MARTIN DREXHAGE
Project Engineer

APPROVED: Clarence D. Turner

CLARENCE D. TURNER
Acting Director
Solid State Sciences Division

FOR THE COMMANDER: John P. Huss

JOHN P. HUSS
Acting Chief, Plans Office

SUBJECT TO EXPORT CONTROL LAWS

This document contains information for manufacturing or using munitions of war. Export of the information contained herein, or release to foreign nationals within the United States, without first obtaining an export license, is a violation of the International Traffic in Arms Regulations. Such violation is subject to a penalty of up to 2 years imprisonment and a fine of $100,000 under 22 U.S.C 2778.

Include this notice with any reproduced portion of this document.

If your address has changed or if you wish to be removed from the RADC mailing list, or if the addressee is no longer employed by your organization, please notify RADC (ESM) Hanscom AFB MA 01731. This will assist us in maintaining a current mailing list.

Do not return this copy. Retain or destroy.

(10) James A./Harrington Roger R./Turk
D. M./Henderson Arlie/Standlee

UNCLASSIFIED

SECURITY CLASSIFICATION OF THIS PAGE (When Data Entered)

(19) REPORT DOCUMENTATION PAGE

READ INSTRUCTIONS BEFORE COMPLETING FORM

(18) 1. REPORT NUMBER: RADC-TR-80-290	2. GOVT ACCESSION NO.: AD-A094 322
	3. RECIPIENT'S CATALOG NUMBER:
(6) 4. TITLE (and Subtitle): INFRARED FIBER OPTICS	(9) 5. TYPE OF REPORT & PERIOD COVERED: Final Technical Report 14 Apr 78 — 12 Apr 80
	6. PERFORMING ORG. REPORT NUMBER: N/A
7. AUTHOR(s): J.A. Harrington R.R. Turk D.M. Henderson A. Standlee	(15) 8. CONTRACT OR GRANT NUMBER(s): F19628-78-C-0109
9. PERFORMING ORGANIZATION NAME AND ADDRESS: Hughes Research Laboratories 3011 Malibu Canyon Road Malibu CA 90265 (12) 172600	(16) 10. PROGRAM ELEMENT, PROJECT, TASK AREA & WORK UNIT NUMBERS: 61102F 2306J130 (17) J1
11. CONTROLLING OFFICE NAME AND ADDRESS: Deputy for Electronic Technology (RADC/ESM) Hanscom AFB MA 01731	12. REPORT DATE: September 1980
	13. NUMBER OF PAGES: 94 (12) 84
14. MONITORING AGENCY NAME & ADDRESS (if different from Controlling Office): Same (11) Sep 80	15. SECURITY CLASS. (of this report): UNCLASSIFIED
	15a. DECLASSIFICATION/DOWNGRADING SCHEDULE: N/A

16. DISTRIBUTION STATEMENT (of this Report)

Approved for public release; distribution unlimited

17. DISTRIBUTION STATEMENT (of the abstract entered in Block 20, if different from Report)

Same

18. SUPPLEMENTARY NOTES

RADC Project Engineer: Martin Drexhage (ESM)

19. KEY WORDS (Continue on reverse side if necessary and identify by block number)

Infrared fibers
Fiber optics
Infrared materials
Light scattering
IFF

20. ABSTRACT (Continue on reverse side if necessary and identify by block number)

This final report summarizes a two-year research program to fabricate optical fibers that are transmissive between 1 and 12 μm. The ultimate goal of this program is to prepare infrared (IR) transmitting fibers with losses less than 5 dB/km. In preparing IR fibers with these low losses, we emphasized the extrusion of very pure KCl as this material has demonstrated bulk losses equal to or less than 5 dB/km in the 2- to 6-μm region. Unfortunately, we were not able to extrude bulk KCl into fiber

DD FORM 1 JAN 73 1473 EDITION OF 1 NOV 65 IS OBSOLETE

UNCLASSIFIED

SECURITY CLASSIFICATION OF THIS PAGE (When Data Entered)

172600

with losses even approaching the goal. During the two-year program, we improved our KCl fiber from an initial loss of 20,000 dB/km to a best value of 4,200 dB/km.

The exceptionally high losses in extruded KCl fiber resulted from the poor surface quality of the fiber. During the extrusion process, the friction between the die and fiber resulted in fibers whose surfaces were highly irregular (fish-scale appearance). Although lubricants alleviated this problem, we found that the fibers still had poor transmission because the lubricants (polymers, in general) could not be completely removed. Extrusions (without lubricants) using different die materials, die shapes, temperatures (25 to 30°C), and extrusion rates (1 mm/hr to 1 cm/sec) did not improve the overall quality of the fiber's surface. To date, we have not been able to develop any experimental conditions which allow us to extrude low-loss KCl fibers and, therefore, we are forced to conclude that KCl and alkali halides in general are not extrudable into transparent IR fibers.

Having reached this conclusion, we began, in the latter states of the program, to develop new fiber fabrication techniques. Two methods seemed most promising. One method, hot-rolling, has the advantage of reduced friction between the fiber and roller surface. The other, single-crystal fiber growth, is designed to produce the ultimate low-loss fiber (ideally no scattering centers). Since these techniques were developed late in the program, only a few preliminary results were obtained. Hot-rolling appears to give good surface quality in KCl reduced from 0.21 to 0.15 in. in diameter.

Our evaluation studies, in addition to the measurement of fiber losses, emphasized the investigation of scattering losses in single- and polycrystalline bulk KCl. By measuring the Rayleigh-Brillouin spectra of KCl, we found that the scattering losses in polycrystalline KCl were not nearly as large as originally expected (about a factor of 5 greater than in single crystals).

This report also summarizes our efforts to fabricate an IR fiber receiver for the detection of pulsed CO_2 laser radiation. This prototype device, which is used in an identification friend or foe (IFF) application, was successfully field tested in Germany.

EVALUATION

This report describes the results of a two-year research effort to develop low loss optical fibers suitable for use in the IR. Although the desired goals of low IR attenuation was not achieved, this work has provided a useful insight concerning loss mechanisms and fabrication techniques applicable to polycrystalline materials such as KCl and KRS-5. The extrusion and hot-rolling methods developed in the course of this program may lend themselves to the production of short lengths of IR transmitting fiber required in a number of military systems and devices. Future efforts in the field of long wavelength fiber materials will benefit from the detailed studies of Rayleigh-Brillouin scattering carried-out as part of this work.

MARTIN DREXHAGE
Project Engineer

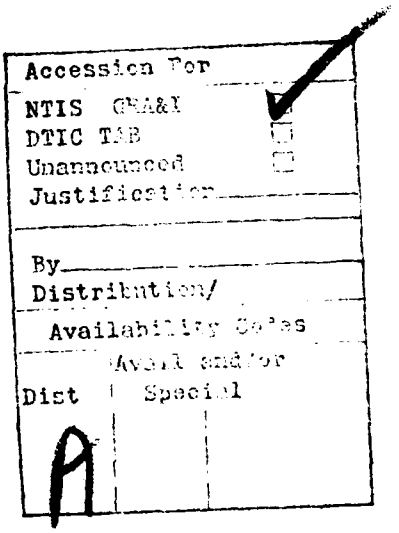

PREFACE

This final technical report describes work on infrared fiber optics performed during the period 14 April 1978 to 12 April 1980. In this report, emphasis is placed on work completed during the last year of the program; the first year's effort is thoroughly covered in the Interim Technical Report issued in July 1979.

The program manager was James A. Harrington, and the principal investigator was Anthony L. Gentile. Overall program coordination was provided by Morris Braunstein and Douglas A. Pinnow (during the first year).

This program has involved the efforts of the following personnel: Arlie Standlee extruded the alkali halide fibers; Roger Turk and Nelson Ramirez made the mechanical measurements, prepared the billets, and made the microphotographs of the surface and subgrain structure; and Bradley Bobbs, Rubin Braunstein, and Jim Harrington performed the optical evaluation studies.

TABLE OF CONTENTS

LIST OF ILLUSTRATIONS

SECTION 1

INTRODUCTION AND SUMMARY

Fiber-optic waveguides that transmit at infrared (IR) wavelengths have numerous applications in sensor and communications systems. Near-term uses of IR fibers include:

- The dissection of images in the focal plane for enhanced detection and signal processing with focal plane arrays
- The relay of focal planes to remote photodetectors
- Flexible transmission of high-power CO and CO_2 laser beams for heating and machining in remote or inaccessible locations.

More long-term applications of these unique waveguides may take advantage of the extremely low loss projected for IR fibers to fabricate long (thousands of kilometers) communications links without the need for optical repeaters. The primary objective of this research program was to develop a new class of fiber-optic waveguides that has the potential for loss well below that of conventional silica fibers. Since the projected losses for IR fiber materials such as the alikali and thallium halides are near 10^{-3} dB/km at 5 μm, the realization of these losses would greatly affect future communcations systems. In this research program, we emphasized the development of KCl fibers, with the more modest goal of 5 dB/km, as the best approach in achieving the ultimate low-loss fiber.

The development of highly transparent IR fibers falls logically into three categories:

- Selection and growth of low-loss materials
- Development of fiber fabrication techniques
- Evaluation of fiber and bulk materials.

Our selection of an appropriate material was aided by our extensive past research and development efforts in the field of highly transparent IR laser window materials. Based on those studies, we chose KCl to emphasize because we had measured losses in bulk KCl single crystals of $5 \pm 5 \times 10^{-7}$ cm^{-1} at 5 μm,[1] even now the lowest loss yet measured in an IR-transparent solid. Therefore, we felt that this highly purified material would be the most promising candidate for fabricating good-quality IR fiber. We initially chose extrusion as the fabrication technique because this method, as developed in our laboratory,[2-4] had been so successfully applied to the Tl halides. Alternative techniques, such as hot rolling and single-crystal growth, were suggested later and only limited results were obtained using these methods. Finally, we evaluated the bulk and fiber materials both optically and mechanically. The optical evaluation included total loss, absorption, and scattering measurements, while mechanical evaluation primarily involved measurements of the fiber's structural features (i.e., surface quality and grain size) and some limited tensile testing.

The results of our KCl extrusion experiments (reviewed in detail in Section 2) were not encouraging. The lowest loss measured at 10.6 μm for a KCl fiber was 4,200 dB/km — far from the program goal of 5 dB/km. These losses are primarily due to the poor surface quality of extruded KCl fiber. Although we tried several approaches to improving the surface quality (such as the use of lubricants, high-temperature extrusion, and long-bearing dies), no good-quality, low-loss KCl fiber could be extruded. We are forced to conclude, therefore, that the extrusion of KCl is not an effective means of fabricating low-loss fiber.

The research program carried out during the past two years was organized into three related tasks:

- Fiber fabrication
- Evaluation
- BIFF (battlefield identification friend or foe).

These tasks and our conclusions are summarized below. The BIFF task was devoted to fabricating a special IR fiber receiver for detecting

pulsed CO_2 TEA laser radiation. This device was constructed and tested (both in the laboratory and in the field) during the first year of the program, and the results are summarized in the Interim Technical Report (issued July 1979). No further work was done on this task during the second year.

A. FIBER FABRICATION

During the past two years, over 30 KCl extrusions were made under a variety of experimental conditions. The extrusion temperature was varied from 25°C to 740°C (KCl melts at 790°C), and the extrusion rates used varied from extremely slow (1 mm/hr) to fast (2 cm/sec). The best-looking fiber resulted when the temperature was near the recrystallization temperature (280°C for KCl) and the extrusion speed was the slowest. This ultra-slow extrusion, although of little practical value, did reinforce our view that the friction between the die and the KCl was the major factor affecting the surface quality of the fiber. That is, fiber extruded very slowly was better than fiber extruded more rapidly because the surface had more time to self-anneal or reconstitute itself. We also found that better surface quality resulted when lubricants (the best was Parafilm M) were used to reduce the friction between the die and the KCl. The major problem with lubricants is that they are, in general, organic polymers that, because their absorption at 10.6 μm is unacceptably high, must be removed after extrusion. The high absorption of the lubricant also means that lubricants are not satisfactory as a cladding even if one could find a lubricant with a refractive index less than that of KCl (n=1.45 at 10 μm). The surfaces of extruded KCl fiber were also quite poor when different die shapes, die materials, and reduction ratios were used.

The difficulties in fabricating KCl fiber by extrusion might be overcome by using the techniques of hot rolling and single-crystal fiber growth. Toward the end of this program, we were able to obtain some preliminary data on hot rolling polycrystalline KCl fibers. We found that the small reductions in area and lower friction inherent in the rolling process enabled us to satisfactorily reduce KCl with good surface quality. Although we have not yet fabricated small-diameter fibers, these results are encouraging and we feel that this technique holds promise for fiber fabrication. Although single-crystal fiber growth has not yet been successful, we feel that this method may

ultimately yield the best-quality fiber since scattering losses should be minimized in this type of waveguide.

B. EVALUATION

Optical and mechanical evaluation of the bulk, billet, and fiber material was carried out on a selective basis. The optical measurements were generally carried out at 10.6 μm using our stabilized CO_2 laser for insertion-loss measurements of fibers and the CO_2 laser calorimeter for absorption-loss measurements in bulk and billet materials. Light scattering studies at 488.0 nm gave us information on the attenuation due to scattering in bulk single- and poly-crystalline samples of KCl.

The 10.6-μm insertion-loss measurements of KCl fibers yielded a wide range of absorption coefficients. Our initial extruded KCl fiber had losses in excess of 20,000 dB/km. The best loss attained in this program was 4,200 dB/km for KCl extruded with the lubricant Parafilm M. These losses are primarily due to the poor surface quality of the fiber.

We placed major emphasis during this program on determining the scattering losses in KCl. This is especially important for polycrystalline fiber waveguides where one suspects a priori that scattering resulting from grain boundaries may be particularly intense. From our Rayleigh-Brillouin (RB) scattering studies on bulk single- and polycrystalline KCl, we concluded that scattering is stronger in polycrystalline than in single-crystal materials but often not as intense as we had expected. These results are summarized in Appendix A.

The mechanical evaluation was limited to a few selected strength tests. The strongest KCl fiber had a yield strength of about 1000 psi for an extrusion temperature of 280°C (Parafilm lubricant). Photomicrographs were taken of each fiber to study grain size and surface quality. Grain size varied between 50 and 200 μm. Surface quality, which is a most important property, varied from highly fish scaled (milky appearance) to glassy-looking for the lubricated fibers. Removing the

lubricants often revealed longitudinal striations ("die marks") and etching in HCl, while removing the striations revealed the microcrystalline structure of the fibers.

C. BIFF

During the last few months of the first year's effort, the Army requested that a prototype IR fiber device be fabricated for use as a detector/transmitter of pulsed, TEA-laser (10.6-μm) radiation. In this application, a pulsed (coded) CO_2 TEA laser is used as a source in troop training or BIFF exercises. The detection of this coded information at distances up to 3 km is accomplished using an IR fiber/detector assembly (BIFF device). Specifically, two ∿50-cm-long, 250-μm-diameter KRS-5 (thallium bromoiodide) fibers detect the laser radiation and then transmit the signals to two HgCdTe detectors for processing.

The present BIFF device successfully underwent proof-of-concept testing in NATO field tests conducted in Grafenwohr, Germany during July 1979. Future Army or other DOD systems will involve more complex systems involving arrays of IR fibers for the passive detection of IR radiation. One such application, for which this device is a test model, involves the linkage of CO_2-laser signals impinging on an armored vehicle to a central detector array. In this use, IR fibers would be placed at strategic points on the exterior of the vehicle (such as a tank used in troop-training exercises or BIFF) to receive coded IR signals. The signal would then be transmitted for signal processing via the waveguide to a central cooled detector located in the benign interior of the vehicle. Thus, the IR fibers would serve as simple detectors (which, unlike pyroelectric or other conventional detectors, require no power to operate) for incoming signals. They would also transmit information from a hostile environment (exterior of the vehicle) to an environment in which a central detector may conveniently be linked to signal-processing equipment. In this way, IR fiber waveguides currently under development at HRL may be used to reduce system costs by minimizing the

number of detectors while simultaneously providing a passive fiber link that is resistant to EMI and enemy intrusion.

D. MAJOR ACCOMPLISHMENTS AND CONCLUSIONS

To meet the program goal of 5 dB/km, we chose at the outset to pursue the extrusion of KCl fiber because KCl had demonstrated ultra low loss in bulk, single-crystal form at 5 μm. Before this program, there was essentially no information on extruded KCl or the other alkali halides. But because of our success with the Tl halides (we had shown them to be readily extruded into good-quality — 400 dB/km for KRS-5 (TlBrI) fibers — waveguides at 10.6 μm), we were very optimistic that the alkali halides would similarly yield to the extrusion process. However, neither KCl nor the few other alkali halides selected were found to be extrudable into low-loss fiber.

This program achieved the following major accomplishments:

- The application of extrusion techniques to extrude KCl, CsI, and KBr into fibers from 500 to 1000 μm in diameter.
- The reduction of extruded KCl fiber losses from an initial high of 20,000 dB/km to a best value of 4,200 dB/km.
- The initiation of hot-rolling and single-crystal fiber growth as new methods of fabricating low-loss fibers from KCl or other materials.
- Made the first study of RB scattering from single- and poly-crystalline KCl designed to separate individual scattering to the total attenuation in transparent solids.
- Concluded from RB scattering that scattering is greater in polycrystalline than in single-crystal materials — although not by as much as initially expected.
- Measured the grain size (50 to 1000 μm) and tensile strength of KCl fibers and studied in detail the nature of the surface irregularities in extruded KCl fiber.

- Delivered to ERADCOM the first prototype IR fiber receiver for the detection of coded TEA laser pulses. Device was successfully tested out to a range of 2.7 km in NATO field tests in Germany.

This two-year research program has led us to the following conclusions and recommendations:

- Alkali halides, in particular KCl, are not extrudable into low-loss polycrystalline fibers.

- New methods, such as hot rolling and single-crystal fiber growth, should be tried for fabricating alkali halide fibers. The greatest promise may be in growing single-crystal fiber, as this type of waveguide should have the minimum amount of scattering.

- The best IR fiber waveguides to date, the Tl halides, should be pursued more diligently to reduce their losses. In particular, Tl halide RAP chemistry techniques should be developed to purify these materials, and the new methods (hot rolling and single-crystal fiber growth) should be applied to these materials.

- Polycrystalline fiber waveguides should not be abandoned just because they are polycrystalline, for our scattering results suggest that scattering may not be as large in these materials as initially expected.

SECTION 2

TECHNICAL PROGRESS AND DISCUSSION

A. GENERAL CONSIDERATIONS

In developing highly transparent IR fiber waveguides, one is confronted with a large class of low-loss materials. On the surface, it would appear for the crystalline materials that all 20 of the alkali halides (Group IA-VII) are suitable as are the more ductile Tl and Ag halides. In addition, there are a few special glasses (BeF_2, $ZnCl_2$,[5] and fluoride glasses [6,7]) that may also be suitable for low-loss fibers. For crystalline solids, however, the choice of materials is greatly restricted by practical considerations concerning fabrication techniques. Figure 1 shows the five crystalline materials that have received the greatest attention for IR fiber fabrication to date and gives their transmission ranges. At HRL, we have studied KCl, KBr, TlBr, and KRS-5 (TlBrI); Honeywell has investigated AgCl.[8] Some of the physical properties of these five materials that have a bearing on the fiber-making process are displayed in Table 1. The Tl and Ag halides have the desirable properties of low solubility and low melting point (greater ductibility), but they have high indices of refraction (greater scattering). In contrast, the alkali halides have low refractive indices but high melting points and rather high solubilities. All these materials are cubic, which is probably necessary to minimize scattering in the polycrystalline materials.

A more detailed analysis of the properties of the 20 alkali halides has been compiled and is shown in Table 2. Looking first at the melting points (M_p) and solubilities, CsI appears to be a good candidate because of its lower M_p and greater ductibility. Unfortunately, most of the other alkali halides are less promising than KCl, KBr, or NaCl because of higher M_p, greater solubility, or insufficient transparency in the IR (such as the Li salts). Therefore, since we had available highly purified, RAP-grown KCl, KBr, and NaCl, we decided to work

Table 1. Properties of IR Fiber Material

9508–10

PROPERTY / MATERIAL	n (10 μm)	M_P, °C	SOLUBILITY, g/100g H_2O
KRS–5 (TlBrI)	2.37	414	5.0×10^{-2}
TlBr	2.34	460	4.8×10^{-2}
AgCl	1.98	455	1.5×10^{-4}
KBr	1.52	730	65.2
KCl	1.45	790	34.3

NOTE: ALL MATERIALS ARE CUBIC

Table 2. Physical Properties of 20 Alkali Halides

IA / VII	Li	Na	K	Rb	Cs
F	M_p = 870°C	992°C	880°C	760°C	683°C
	ρ = 2.60g/cm^3	2.79	2.50	2.88	3.58
	n = 1.35 (3.8 μm)	1.23 (10.6 μm)	1.36 (0.57 μm)	1.35 (10 μm)	1.44 (10 μm)
	Hardness = 102 (Knoop)	60			
	Solubility = 0.27g/100g H_2O	4.2g/100g H_2O	92.3g/100g H_2O	130.6g/100g H_2O	367g/100g H_2O
Cl	M_p = 614°C	800°C	790°C	715°C	460°C (tr); 646 (β)
	ρ = 2.06g/cm^3	2.16	1.99	2.76	3.988
	n = 1.53 (10 μm)	1.48 (10 μm)	1.45 (10.6 μm)	1.47 (10 μm)	1.61 (10 μm)
	Hardness =	18	8		
	Solubility = 63.7g/100g H_2O	36g/100g H_2O	34.3g/100g H_2O	77g/100g H_2O (0°)	186g/100g H_2O
Br	M_p = 547°C	755°C	730°C	682°C	636°C
	ρ = 3.46g/cm^3	3.21	2.75	3.35	4.43
	n = 1.69	1.58 (10 μm)	1.52 (10.6 μm)	1.52 (10 μm)	1.66
	Hardness =		7		19.5
	Solubility = 63.7g/100 g H_2O	91g/100g H_2O	65.2g/100g H_2O	98g/100g H_2O (5°)	124g/100g H_2O
I	M_p = 446°C	651°C	723°C	642°C	621°C
	ρ = 4.06g/cm^3	3.66	3.11	3.55	4.51
	n = 1.92	1.72 (10 μm)	1.62	1.61 (10 μm)	1.74 (10 μm)
	Hardness =				5
	Solubility = 165g/100g H_2O	179g/100g H_2O	144g/100g H_2O	152g/100g H_2O	44g/100g H_2O (0°C)

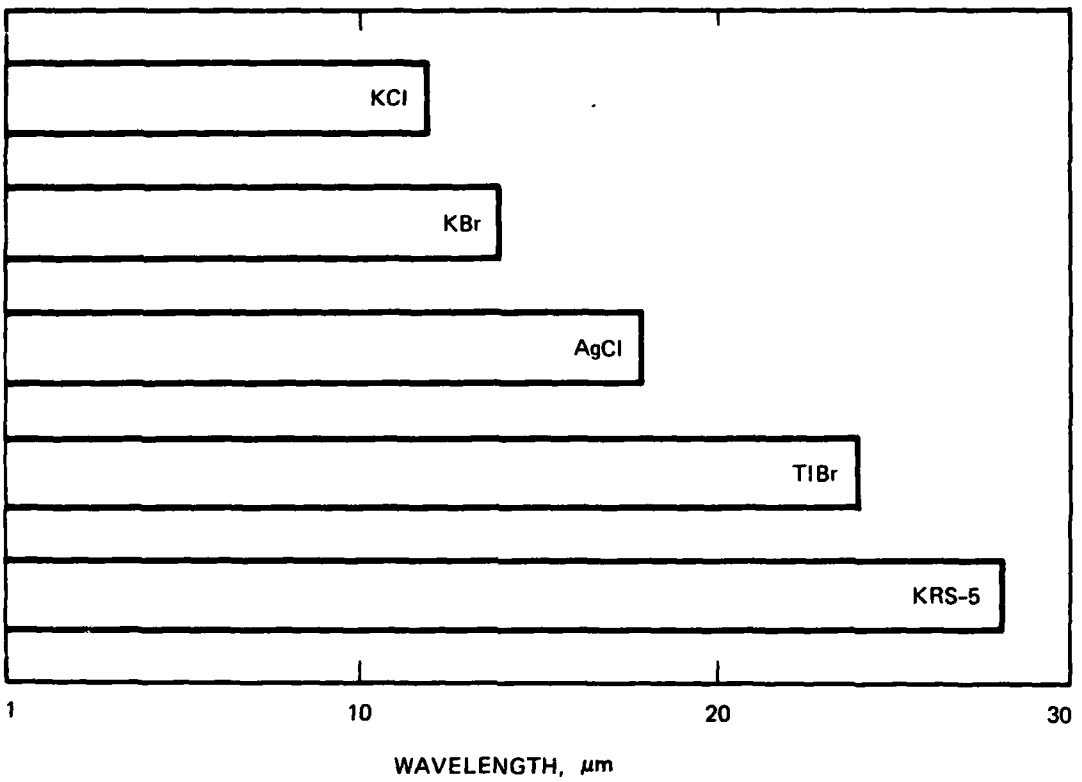

Figure 1. Transmission range of polycrystalline IR fiber materials.

primarily with these salts rather than to experiment with less well characterized and less understood alkali halides. In addition, we felt that KCl had demonstrated the lowest loss in bulk form[1] and we felt it to be the cleanest salt.

The ultra low loss potential of these salts has been discussed by several investigators.[3-5] We recently calculated the projected loss for KRS-5; this result and those for KCl and fused silica (for reference) are shown in Figure 2. At short wavelengths, the attenuation curves are those calculated from scattering losses (decreasing as λ^{-4}), while at the long wavelengths the attenuation is bounded by multiphonon (lattice) absorption. The characteristic V shape of these crossed curves clearly indicates that the minimum in KCl or KRS-5 (or related IR transparent solids) is well below that of fused silica. In fact, the V curve for silica, rather than being merely projected, has been traced out experimentally, and losses of 0.25 dB/km at 1.6 μm (V curve minimum) have been achieved in kilometer-long fiber.[9] The important point to emphasize about these curves is that the projected losses are very low ($\sim 10^{-3}$ dB/km) for crystalline solids and that KCl and KRS-5 are only two of many such materials having this potential.

B. FIBER FABRICATION.

1. Extrusion Mechanics and Lubricants

Extrusion methods have been used for the past three years to successfully fabricate KRS-5 and TlBr fibers. Polycrystalline fibers of these Tl-containing salts were prepared with losses as low as 300 dB/km (KRS-5). In this program, we decided to pursue the extrusion of KCl because KCl has measured losses that are considerably better than those of KRS-5.

The extrusion process has worked well for the Tl-containing salts, in part because of the easy plastic deformation of these materials.

9467-1

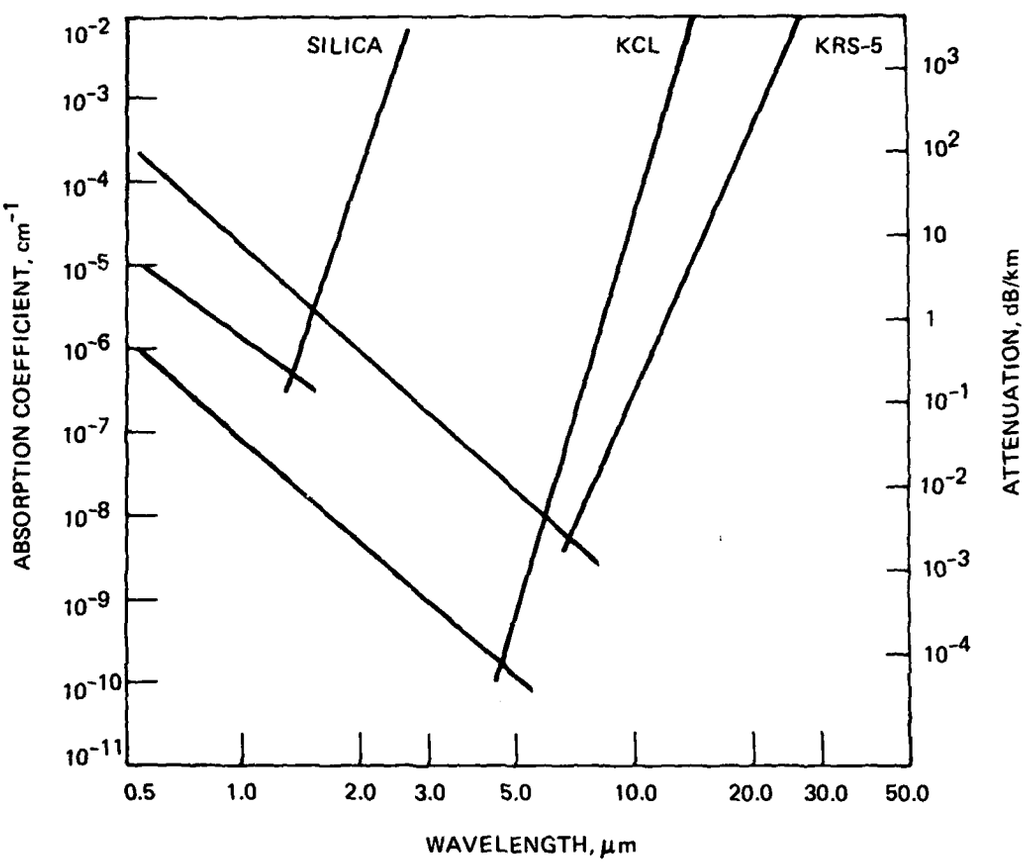

Figure 2. Projected transmission in infrared fibers.

Harder materials like KCl, NaCl, and KBr have proven more difficult to extrude owing to their higher melting points. The higher melting points (>700°C) mean greater friction between the diamond die and billet, which results in extruded fiber with many surface irregularities. In our KCl extrusions, for example, to reduce the 5.5-mm starting billet to a 500-μm-diameter fiber requires an area reduction of 120:1. Therefore, as the material passes through the die, the billet's axis region must move 120 times faster than its outer shell. This shears out a core from the billet, the surface of which must be smoothly reconstituted as it passes through the die. This readily occurs for KRS-5 but not for KCl.

The use of lubricants in extrusion reduces the friction between the die and fiber. During this program, over a dozen different lubricants were tried, but only Parafilm M was found to be a good lubricant. In general, the lubricants were chosen on the basis of being easily removed from the KCl, which meant that our choice was limited to waxes and greases. Unfortunately, those materials have low melting points and the lubricant usually pressed up along the piston rather than being coextruded on the fiber's surface.

Although lubricants such as Parafilm M do improve the surface quality of the resultant fiber, they would not be a good long-term solution to producing low-loss fiber. The reason is that almost every material that can act as a lubricant is difficult to remove completely from the KCl after extrusion. The search for lubricant/cladding combinations is very limited since the cladding requirement imposes an additional low index of refraction (<1.45) and high transparency requirement on the lubricant.

The results of the extrusion runs made during the last year of the program are given in Table 3. The earliest runs involved lubricants (the last attempts to produce a good fiber using this technique), and all fibers were extruded using a 500-μm-diameter die made from either diamond or tungsten carbide. A surfactant (wetting agent) was added to beeswax in run no. 72 to improve beeswax's ability to stick to KCl.

Table 3. KCl Extrusion Runs

Date	Run No.	Sample No.	Temperature °C	Comments
8-23	72	B154-2-7	220 270 300	Beeswax plus surfactant
8-30	74	B176-1	225	Parafilm M plus Ni powder
9-27	79	B176-1	170 200 280 350	No lubricant, fiber extruded into Cereclor 42
9-28	80	B176-2	170 200 270 350	Carbide die, no lubricant
10-4	82	B176-2	100 120 130	No lubricant
11-9	87	B154-2	300	No lubricant, very slow extrusion
11-24	93	--	300 400 738	No lubricant, long-bearing carbide die

Unfortunately, the beeswax did not wet the KCl any better with surfactant than without it. The beeswax appeared only on the first few inches of extruded fiber.

A potentially severe problem with lubricants is swirling of the lubricant into the fiber core (making complete removal of the lubricant impossible). To monitor the extent that Parafilm M was carried into the core, we impregnated the Parafilm M with Ni particles prior to wrapping the lubricant on the KCl billet (run no. 74). After the fiber was extruded, we cross-sectioned the fiber and examined the ends under the microscope. We found, as expected, Ni particles in the

core of the fiber. Generally, the Ni plus lubricant would be in indentations around the core perimeter at depths of 10 to 20 μm into the core. We conclude from this experiment that the lubricant mixes with core material and, therefore, that using lubricants in extrusion cannot help us produce low-loss fiber.

We felt that one reason for the fish-scale surface of the extruded KCl was attack of the KCl surface by moisture in the air. Since after run no. 74 (Ni particles plus Parafilm M lubricant) we had decided to abandon lubricants to study unlubricated KCl, we decided first to investigate the extrusion of KCl into a moisture-free environment. We hoped that this would eliminate the weakened surface that results from attack by water, leaving us with a smooth fiber surface.

To create a water-free environment immediately after the extrusion die, we decided to extrude into Celeclor. This oily liquid absorbs moisture and in so doing generates small amounts of chlorine; also, it does not react with KCl. In effect, this liquid acts as a RAP atmosphere[10] and prevents moisture from reaching the surface of the KCl. A special tube, shown in Figure 3, was filled with Cereclor and pushed up under the die so that the fiber exiting the die would immediately contact the Cereclor.

The results of run no. 79, the extrusion of a 500-μm-diameter KCl fiber into Cereclor, are seen in the 100X microphotographs shown in Figures 4 through 6. A variety of extrusion parameters were used in an attempt to achieve the best surface quality. The start of run no. 79 into Cereclor was done at 170°C at a very slow extrusion rate (∿1 in./min). After the Cereclor was removed, we see in Figure 4 that the surface of this fiber is poor. Subsequent low speed extrusions at 200, 280, and 350°C (Figures 4 and 5) yielded even worse surface quality. The characteristic fish-scale appearance is readily seen in these photographs. Figure 6 compares, for the fast extrusion rate of ∿1 in./min, two 350°C extrusions of KCl: one into Cereclor and one into air.

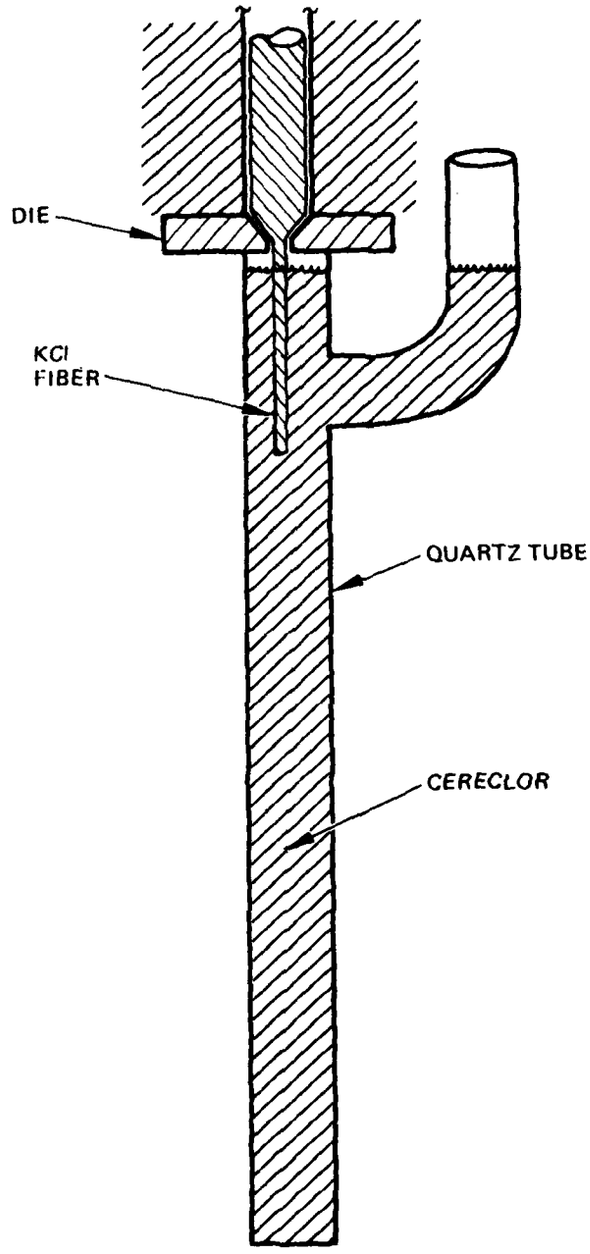

Figure 3. RAP (Cereclor) environment to protect fiber's surface from attack by moisture.

9888-8

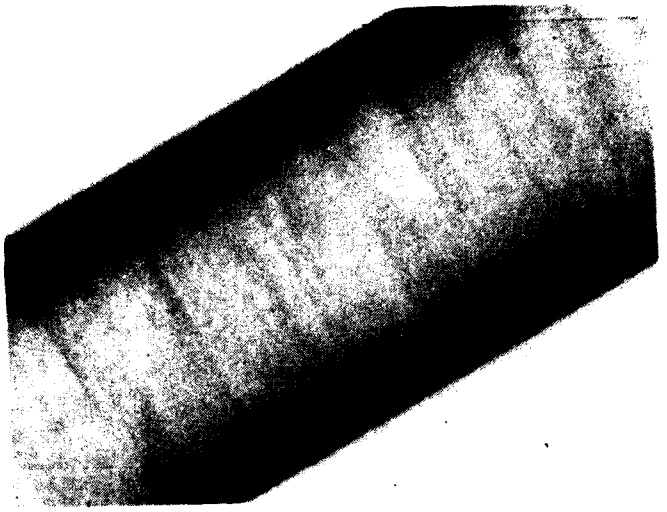

Figure 4(a). Extruded at 170°C in Cereclor 42P at low speed.

9888-9

Figure 4(b). 100X, extruded at 200°C in Cereclor 42P at low speed.

9888 4

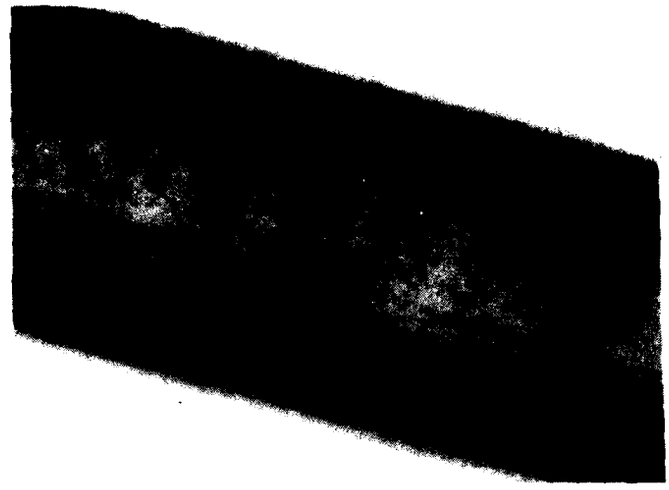

Figure 5(a). 100X, extruded at 280°C in Cereclor 42P at low speed.

9888-5

Figure 5(b). Extruded at 350°C in Cereclor 42P at low speed.

9888 6

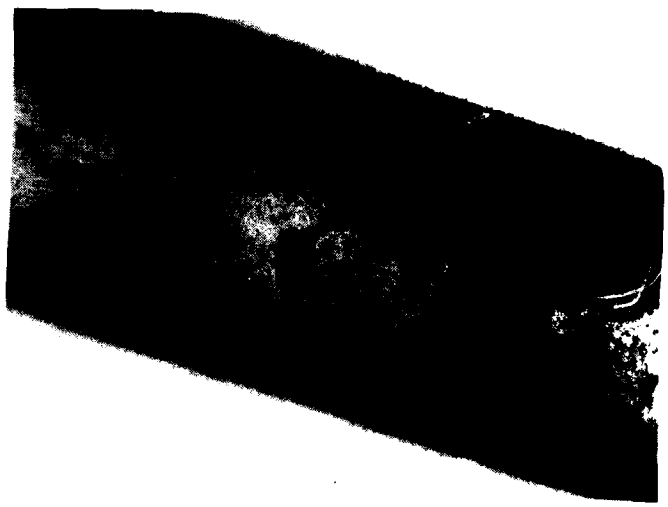

Figure 6(a). 100X, extruded at 350°C in Cerecler 42P at high speed.

9888-7

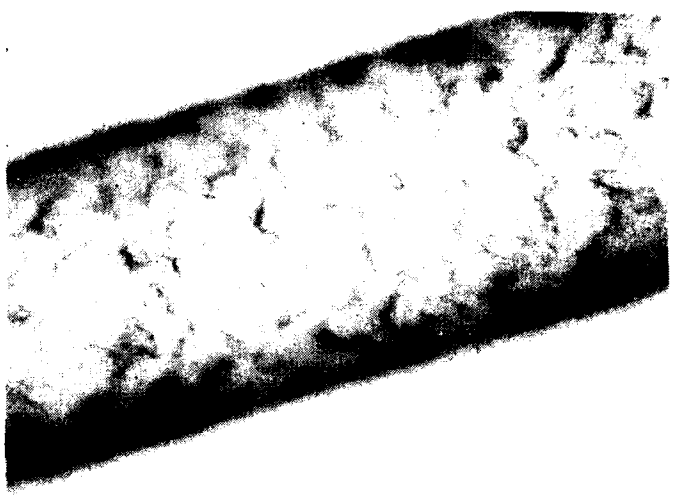

Figure 6(b). Extruded at 350°C into air — no Cereclor — at high speed.

Both surfaces are fish-scaled, although the fiber extruded into Cereclor is somewhat less so. These measurements forced us to conclude that the absence of moisture did not significantly improve the quality of the KCl fiber.

2. Effect of Different Extrusion Dies

In an attempt to improve the surface quality of the KCl fiber, dies with shapes different from the characteristic donut shape of the diamond dies were tried. There were two attempts. The first (run no. 80) used a tungsten carbide (WC) die with a venturi shape for a gentle reduction; the other (run no. 93) used a long-bearing, WC die so that the KCl would be reconstituted or self-annealed in a uniform, hot region after reduction.

In run no. 80, the gentle reduction of the KCl was accomplished using the WC die sketched in Figure 7. The diameter of the extruded fiber was 500 μm. With a temperature range varying from 170 to 350°C and extrusion rates from slow (∿1 in./hr) to fast (∿1 in./min), the fiber surfaces again appeared fish-scaled. Figures 8 through 10 show the poor surface quality of KCl resulting from this WC die and extrusion into air (no lubricant used). The surface of the 170° extrusion was the best (note grain size in 200X photo in Figure 8). At the higher temperatures of 200 and 270°C (Figure 9) and 350°C (Figure 10), the surface was fish-scaled. This die has thus not alleviated our surface irregularities.

For run no. 93, to prevent the shearing of the KCl fiber surface, we designed a WC die (Figure 11) that we hoped would reconstitute or self-anneal the KCl surface. The length of this die was made long in comparison to its cross section so that the uniform region would provide a region for smoothing the surface. At extrusion temperatures of 300 and 400°C (no lubricant) and a variety of extrusion rates (run no. 93), we found that the fiber surfaces still remained fish-scaled. We, therefore, concluded that different shaped dies of WC do not help produce smooth surfaces and no further die shapes (or materials) were pursued.

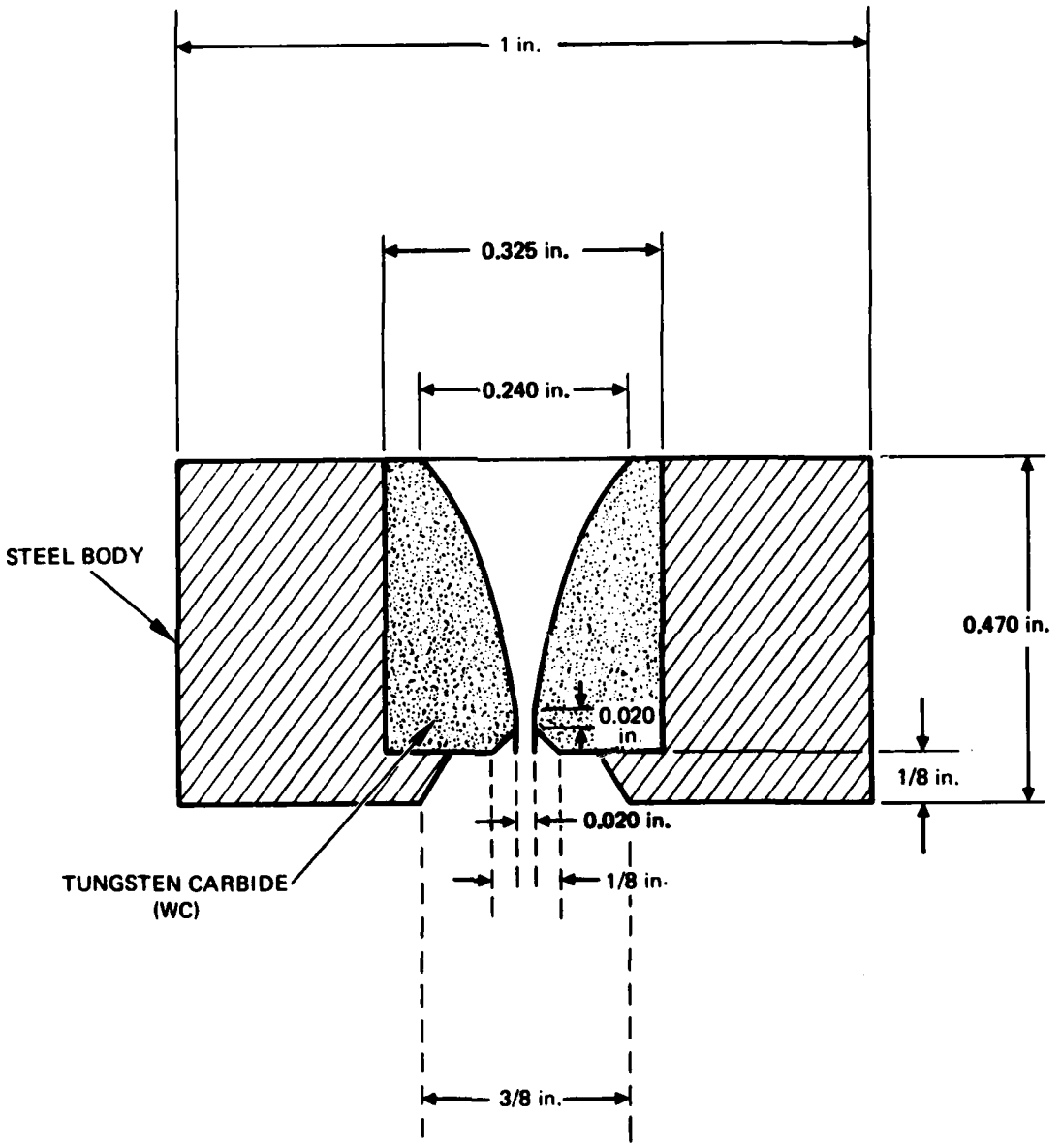

Figure 7. WC die for gentle reduction of KCl.

9888-2

Figure 8(a). 100X, extruded at 170°C, low speed.

9888-3

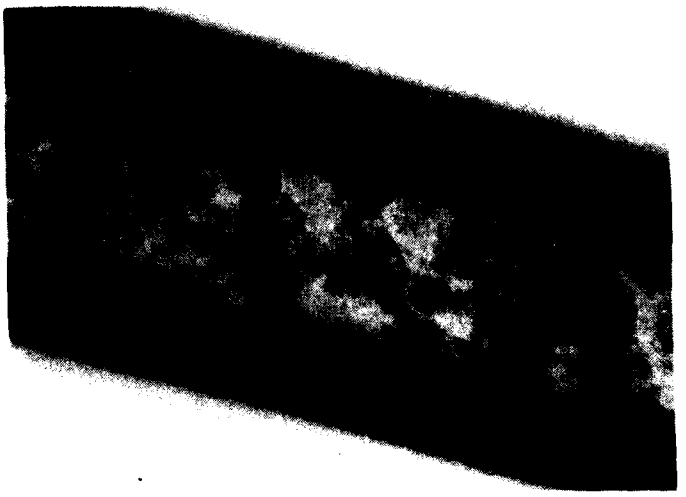

Figure 8(b). 200X, extruded at 170°C, low speed.
Average grain size is 105 μm.

9888-10

Figure 9(a). 100X, extruded at 200°C, low speed.

9888-11

Figure 9(b). 100X, extruded at 270°C, low speed.

9888 12

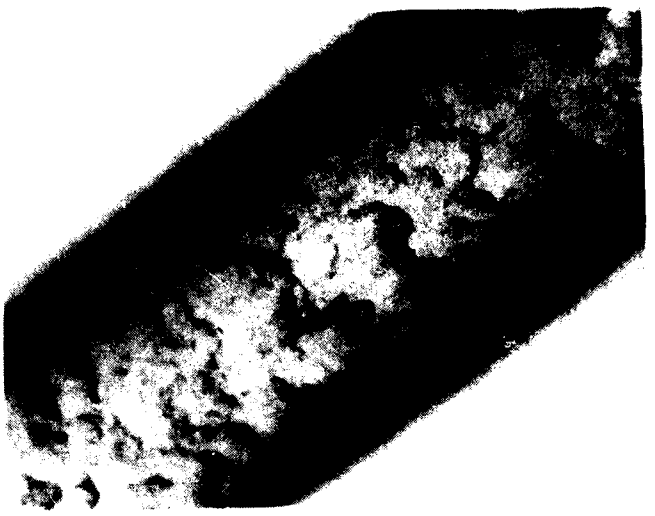

Figure 10(a). 100X, extruded at 350°C, low speed.

9888-13

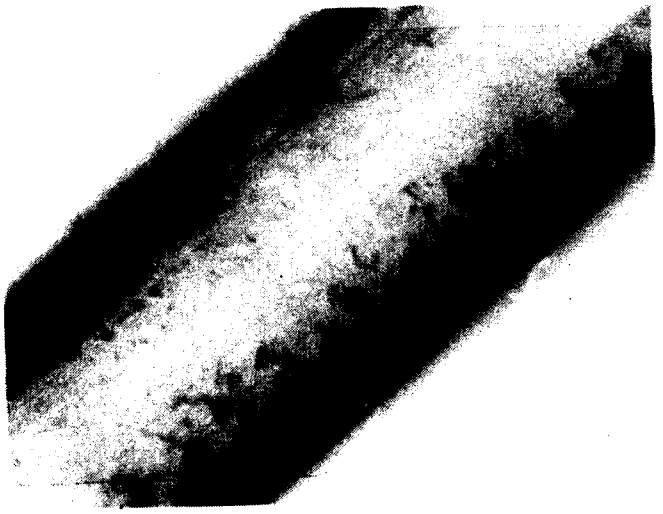

Figure 10(b). 100X, extruded at 350°C, high speed.

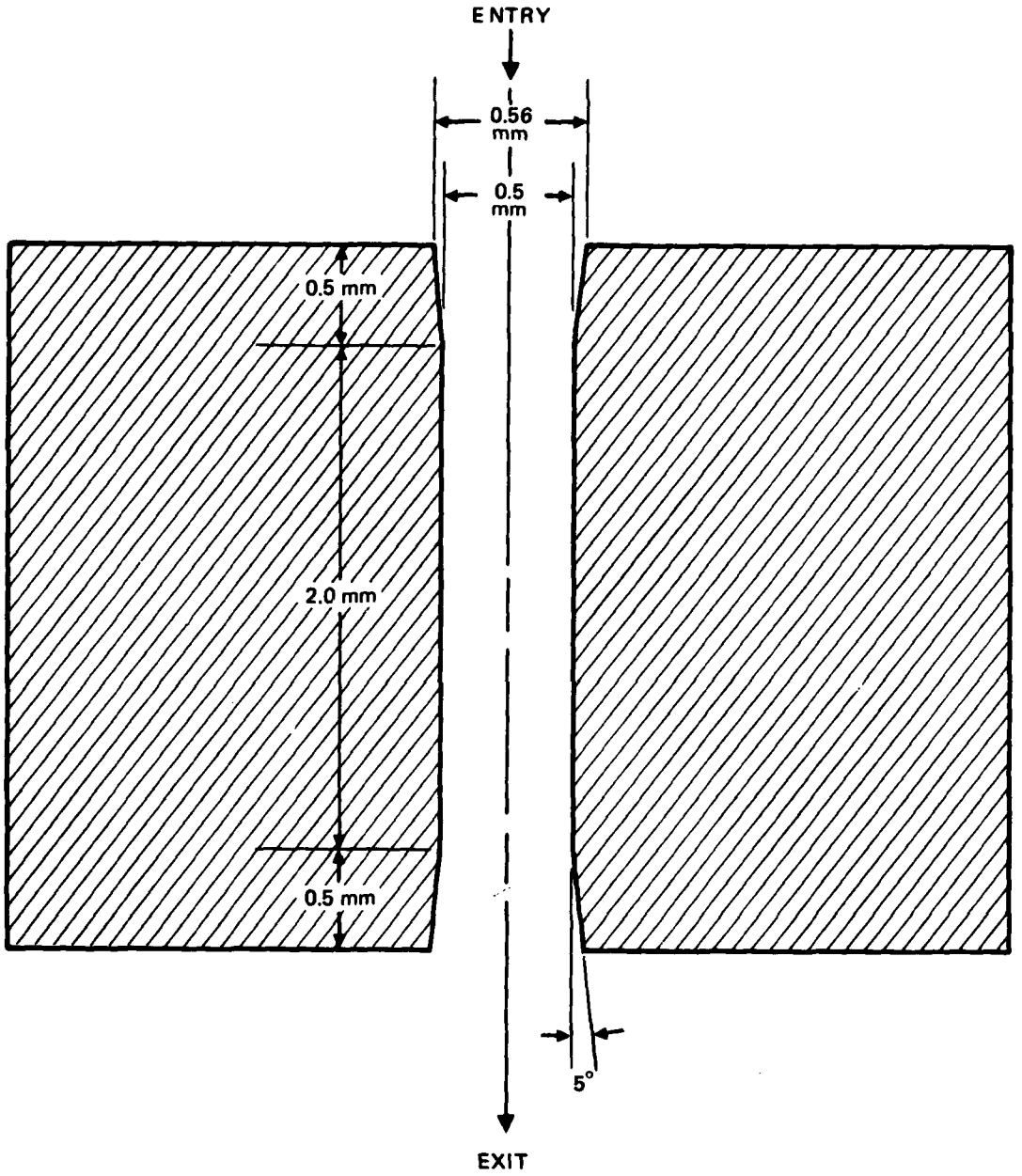

Figure 11. Long-bearing WC die for KCl extrusion.

3. High-Temperature Extrusion

Having determined that using lubricants afforded no long-range solution to our extrusion problems, we decided to minimize friction between die and fiber by going to very high extrusion temperatures. Most of our experiments had been done at temperatures between 170 and 350°C, less than half the 790°C melting point of KCl. To be able to increase the extrusion temperature, we modified our extrusion heater to permit extrusion at temperatures up to 800°C.

The results for unlubricated, 500-μm-diameter KCl fiber (run no. 93) are shown in Figure 12. The long-bearing WC die was used, and the highest extrusion temperature was 740°C. At this temperature, the fiber was still not smooth. Instead, the surface exhibited a shingle-type (layer-type) structure as if the surface material had partially melted and flowed (see Figure 12). The fiber grain size, as expected, was very large (several mm) and the fiber naturally was very brittle. These results led us to conclude that high temperatures would not solve the surface-quality problem.

4. *Effect of Reducing Area Reduction in Extrusion*

The friction between die and fiber may be significantly reduced by minimizing the area reduction. Instead of the 120:1 area reduction used in all of our previous extrusions, we decided to use a 4:1 reduction to determine if such an extremely low value would produce KCl fiber with smooth surfaces. To achieve this 4:1 reduction, we fabricated a WC die to accept our 0.5-in.-diameter KCl billets and reduce them to 0.25 in. in diameter. The heel of a KRS-5 billet, shown in Figure 13, illustrates how the reduction occurred (KRS-5 is shown only for convenience — the same situation applies to KCl). The experiments were carried out on unlubricated KCl at 250°C.

The results of these experiments are shown in Figures 14 and 15. As in the earlier extrusions at higher area reductions, the slowest rate

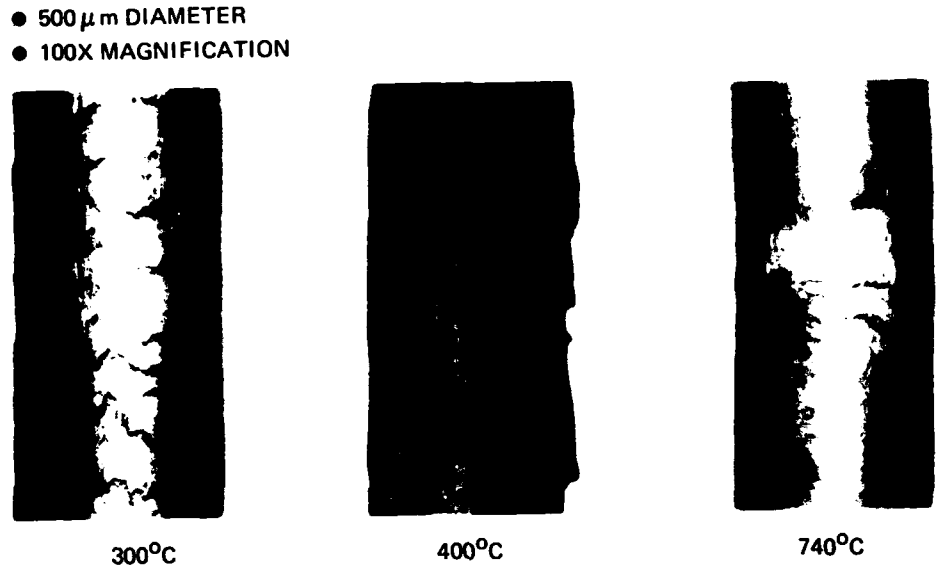

Figure 12. High-temperature extrusion of KCl fiber.

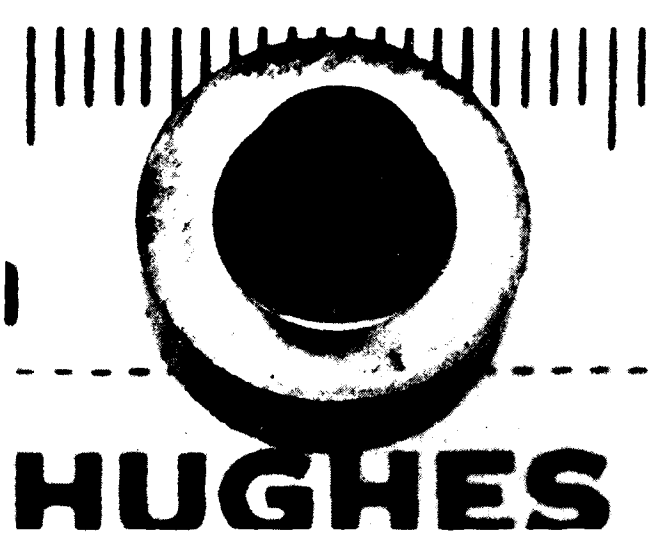

Figure 13. Heel of KRS-5 billet showing 4:1 area reduction used for KCl extrusion.

9888 14

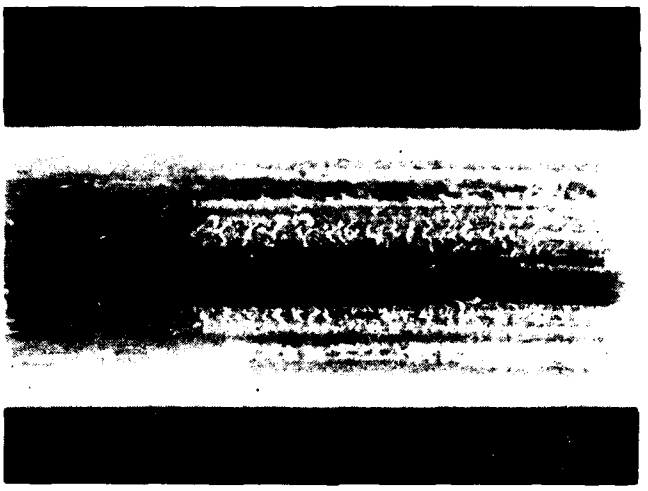

Figure 14(a). 8X, extruded KCl, low rate, 0.25 in. diameter.

9888-15

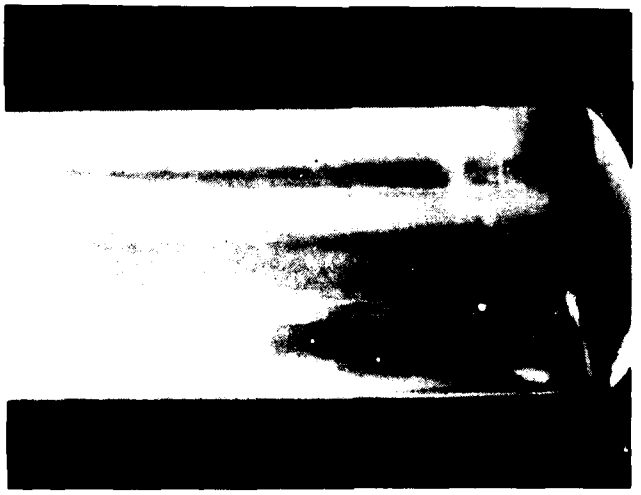

Figure 14(b). 8X, extruded KCl, low rate, 0.25 in. diameter. Right side is first portion out of extruder.

9888 16

Figure 15(a). 8X, extruded KCl, medium rate, 0.25 in. diameter.

9888-17

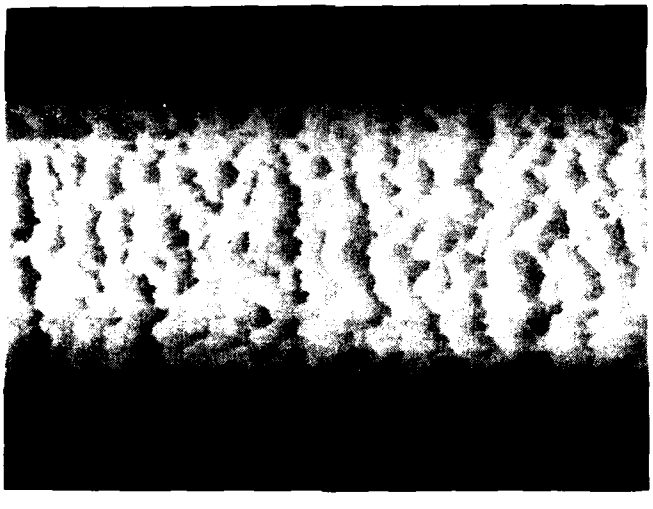

Figure 15(b). 8X, extruded KCl, high rate, 0.25 in. diameter.

produced the best surface quality (longer time to self-anneal). Figure 14 shows this as does the observation that the smoothest surface occurs at the beginning of the extrusion (this has been seen in other extrusions as well). At the higher extrusion rates (see Figure 15), the surface again appears fish-scaled. This was very discouraging for we had hoped that the friction would be enough lower so that a smooth surface would result. If it had been, we could have extended this concept (i.e., small area reductions) to produce small-diameter fibers merely by using a multihole (spinerette) die. Unfortunately, this experiment indicates that nothing would be gained by doing this.

5. Hot-Rolling KCl Fibers

An alternate technique for fabricating fibers is hot-rolling. In this method, the cross section of the KCl is reduced by compressive deformation, as in forging. Potassium chloride windows have been forged successfully to reductions of 93% at temperatures as low as 150°C with no reduction in IR transmission and a 500% increase in strength. Like forging, rolling involves limited frictional contact; the relative movement of rolls and material is at a minimum for reductions of 10 to 20%. In rolling, repeated passes and long lengths are possible. Most important, rolled surfaces closely duplicate the smoothness of the rolls, providing an opportunity to produce fibers with optically smooth longitudinal surfaces. Forming shapes by rolling is common, as in wire rolling, using shaped rolls.

Two problems may occur in rolling. To achieve the temperature needed to deform KCl, about 200°C, a protective atmosphere enclosure and special radiant heaters will be required (in the hot-rolling of steel, steam-heated rolls are used). Rolls, bearings, lubricants, and the housing will experience difficult conditions. A second problem is flashing, or the formation of a thin fin by material being exuded between the closed portions of the rollers, instead of being restricted

to the shaped sections. This should be minimized or eliminated through close-fitting, precise rolls, and smaller reductions per pass.

A jewelry roll was adapted for our hot-rolling experiments. Shown in Figure 16, these rollers were heated (to 300°C) and enclosed in a box containing Ar atmosphere. The rolling speed was controlled by an external motor. The reduction per pass varied from 10 to 20%.

Preliminary rolling reductions of 22% in three passes at 300°C have been made on KCl with no cracking. Surfaces duplicate roll finish and, therefore, the fiber's surface should be excellent with smooth-finished rolls.

C. EVALUATION

1. Optical Evaluation — Scattering

The optical evaluation of both fiber and bulk materials provides the foundation of our understanding of loss mechanisms in transparent solids. Absorption loss measurements are performed on window- and billet-size materials using laser calorimetric methods; conventional insertion-loss techniques using IR lasers are employed for fibers. Scattering losses in bulk and fiber materials are measured by means of a Fabry-Perot interferometer system, from which a spectrum of Rayleigh and Brillouin scatter peaks is obtained. An analysis of this spectrum gives the total scattering attenuation coefficient, as well as some insight into the individual scattering mechanisms.

The emphasis of our optical evaluation has again been on the light scattering measurements. Using our Burleigh Fabry-Perot interferometer with the triple-pass attachment for improved contrast, we measured the RB spectra of several single- and poly-crystalline bulk samples. From the spectra, we have been able to calculate the Landau-Placzek ratio R_{LP} for the samples and thus to estimate the attenuation due to scattering.

9728–2

- HOT ROLLING

  ADVANTAGES

  - REDUCED FRICTION
  - SMALLER REDUCTIONS/PASS

  MATERIALS

  - KCl, KRS-5

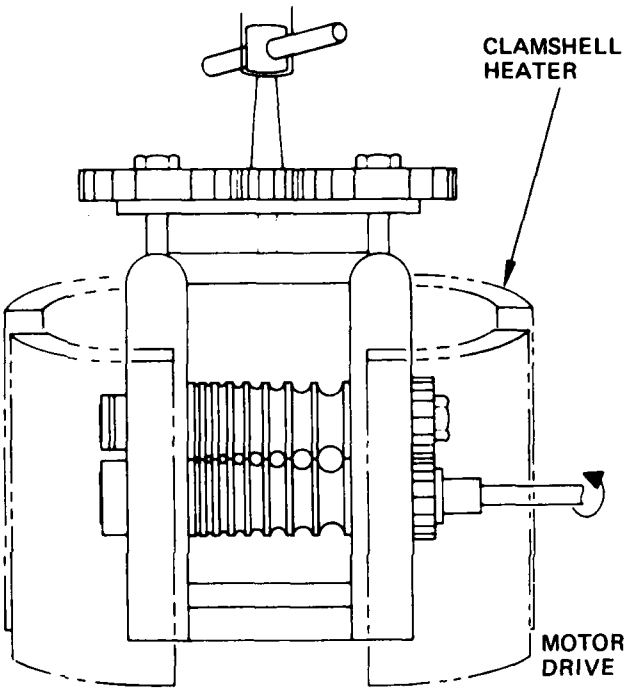

Figure 16. Hot rolling KCl fiber.

The results of our light-scattering measurements recently were presented at the Physics of Fiber Optics Meeting held at the annual American Ceramic Society Meeting (Chicago, Illinois, 28-30 April 1980). A manuscript of this paper has been submitted for publication in the Society's proceedings. This manuscript, which summarizes all our light scattering results, is presented in Appendix A.

2. Optical Evaluation — Absorption

The optical loss measurements were made on bulk, billet, and fiber KCl materials. Although these measurements are summarized in the Interim Technical Report, Table 8 taken from that report is reproduced here as Table 4 to show some of the KCl fiber losses only. These measurements were made using the apparatus shown diagrammed in Figure 17. In Table 4, the insertion loss measurements at 10.6 μm are given for KCl fiber. The lowest-loss KCl fiber measured was 4.2 dB/m. We also note that the fiber losses do not depend strongly on whether the fiber is lubricated or unlubricated. This is somewhat surprising since Parafilm M lubricant has absorption bands at 10.6 μm. The explanation undoubtedly lies in the fact that scattering losses dominate and that the loss in the Parafilm M is small compared to these losses.

The most likely explanation for the high fiber losses is the fiber's poor surface quality. For the unlubricated KCl billets, excessive friction between the die and fiber resulted in a fish-scale surface that often appeared milky in cases of extreme friction. The losses in these fibers were excessive (essentially no transmission over a 25-cm length). The lubricated fibers also had surface irregularities, but not as severe as did the unlubricated ones. For these fibers, the longitudinal striations under the lubricant may have strongly scattered 10.6-μm radiation. When these striations ("die marks") were removed by an HCl etch, which revealed the microstructure, the fibers were still lossy (see Table 4) even though there was no lubricant. In all cases, the surfaces

Table 4. Fiber Losses at 10.6 μm for Parafilm-Lubricated KCl Billets

Date	Run No.	Sample No.	Diameter, μm	Extrusion Temperature, °C	As Extruded, cm^{-1} (dB/m)	Lubricant Off, cm^{-1} (dB/m)	HCl Etch, cm^{-1} (dB/m)
2/2/79	35	B154-7-2	1000	250	2.10×10^{-2} (9.0)	1.70×10^{-2} (7.43)	2.39×10^{-2} (10.4)
2/14/79	36	B154-7-3A	1000	280	1.50×10^{-2} (6.58)	1.50×10^{-2} (6.58)	2.01×10^{-2} (8.73)
		B154-7-3B	1000	200	2.97×10^{-2} (12.9)	1.88×10^{-2} (8.20)	1.88×10^{-2} (8.18)
3/14/79	39	B154-7-4A	500	200	6.53×10^{-2} (28.4)	——	2.71×10^{-2} (11.8)
		B154-7-4B	500	250	1.54×10^{-2} (6.71)	1.52×10^{-2} (6.59)	1.38×10^{-2} (5.99)
		B154-7-4C	500	280	1.16×10^{-2} (5.03)	——	0.96×10^{-2} (4.20)
		B154-7-4D	500	300	1.23×10^{-2} (5.33)	——	1.42×10^{-2} (6.18)
		B154-7-4E	500	350	5.43×10^{-2} (23.6)	——	4.72×10^{-2} (20.5)

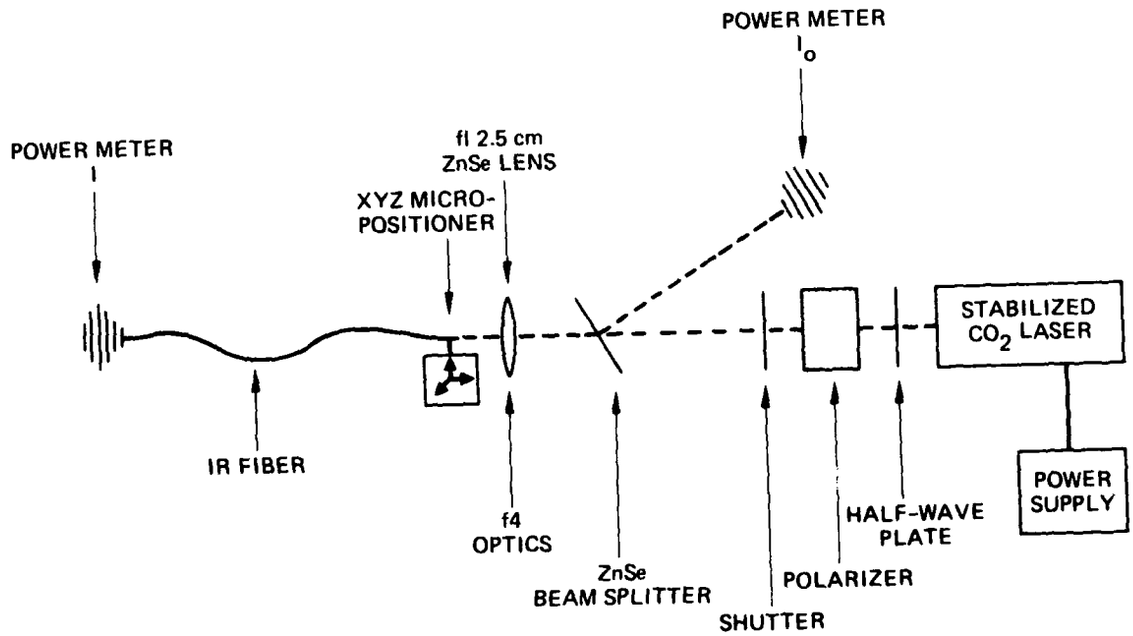

Figure 17. IR fiber loss measurement apparatus.

were rough (with or without lubricant) and thus offered a means for radiation to be scattered out the sides of the fiber. In summary, we feel that if a smooth, clean-surface KCl fiber could be fabricated, the losses in KCl should be at least as good as they are for KRS-5 (10.6 μm absorption, 7×10^{-4} cm^{-1} in the best material).

During the insertion-loss measurements, one determination was made of bulk insertion loss. This was done by selecting a fairly long piece of KCl fiber (27.5 cm), measuring the total loss, and then cutting the fiber into two smaller pieces for loss measurements. When the product of the absorption coefficient β and the fiber length L is plotted versus L, it is possible to obtain the bulk insertion loss (slope) and end surface loss (y intercept). Figure 18 shows our results for 500-μm-dia-diameter KCl fiber with Parafilm M lubricant (B154-7-4, see Table 4). A least-squares fit of βL (total loss) versus L for the three datum points yielded:

$$\beta L = 0.0101L + 0.0108.$$

From this, we obtain a bulk loss of 1.01×10^{-2}cm (4.4 dB/m) and a per surface loss of $0.0108 \div 2 = 0.0054$. This bulk loss is near the minimum loss of 4.2 dB/m (see Table 3), but the surface loss is rather high. Better end finishing would be helpful in minimizing this effect.

For reference purposes, Appendix B presents a paper summarizing our work on Tl halide fibers.

3. Mechanical Evaluation

The mechanical properties of the KCl fibers were studied by measuring the grain size, grain growth, and strength of selected KCl fibers. Since this program emphasized optical properties, few data are available on the tensile strength of the fibers. In general, the extruded fibers were quite brittle and their tensile strength was found to be only slightly greater than that of single-crystal KCl.

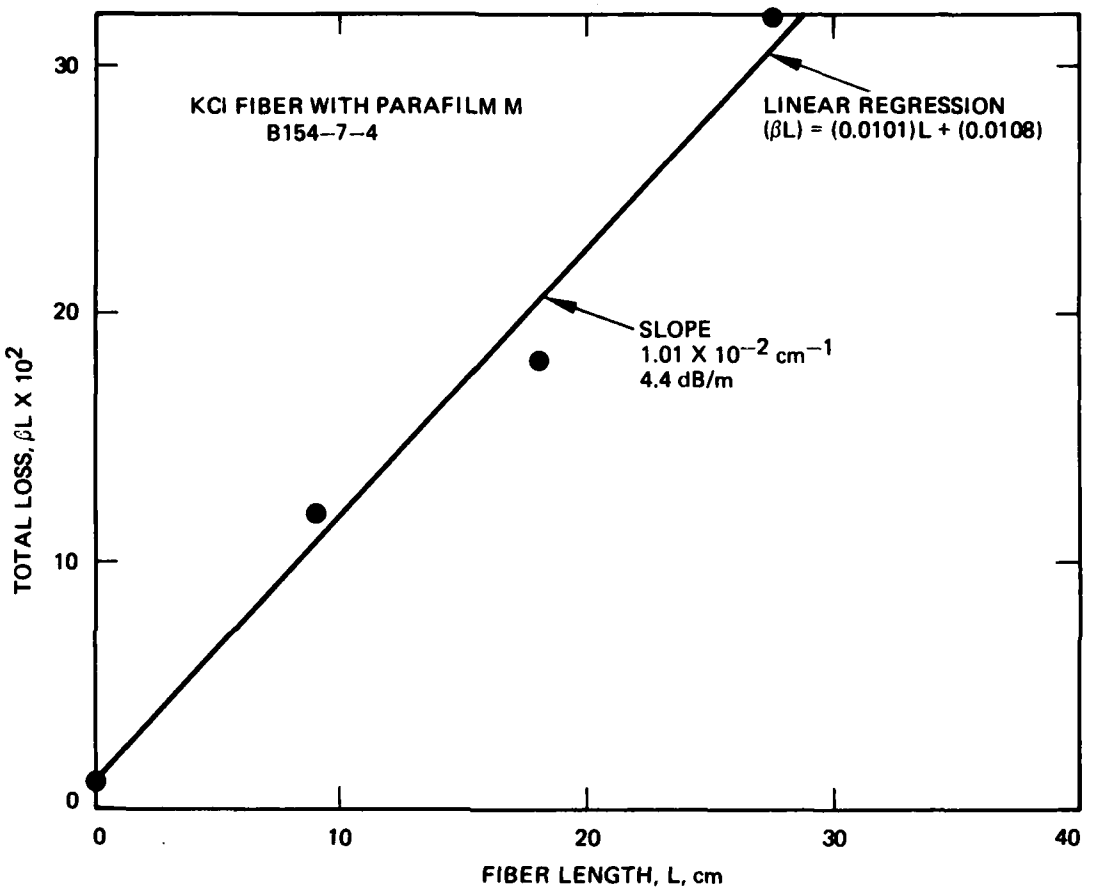

Figure 18. Total loss versus fiber length in 500-μm-diameter KCl fiber.

Tensile testing on 500-μm-diameter KCl fiber coated with Parafilm M was carried out for fibers extruded at several different temperatures. Since we found that fiber grain size decreases with decreasing extrusion temperature, lowering the extrusion temperature implies that strength will be increased. Figure 19 shows these results and the unexpected decrease in strength at the lowest extrusion temperature (200°C). One explanation is that the grains grew (possibly due to moisture), causing the grain size to be larger in this fiber.

D. CONCLUSIONS AND RECOMMENDATIONS

After two years of low-loss IR fiber development, primarily on KCl fiber technology, we are led to conclude that extruded KCl fiber cannot be fabricated to meet the program goal of 5 dB/km. Since our best KCl fiber had losses almost 10^3 greater than this goal, we must turn to alternative fiber fabrication methods and, to some extent, to other fiber materials.

We continue to feel, from a strictly fundamental viewpoint, that KCl fiber should exhibit low loss provided that surface quality (the major limiting loss factor to date) can be improved. In essence, the surface of KCl must appear smooth and free of irregularities; otherwise, we can only expect high losses due to scattering. If a good surface can be obtained, then we feel there is no reason that KCl fiber should not have losses near those of the bulk material ($\sim 10^{-6}\,cm^{-1}$ at 5 μm).[2]

To obtain good surface quality, we recommend the exploitation of hot-rolling and single-crystal fiber growth techniques. Both methods have the potential to produce good surfaces and, for the single-crystal method, there is the additional advantage of fabricating a waveguide virtually free from scattering losses. Our preliminary efforts in hot rolling show promise for this method as the fiber surfaces are as good as the roller's surface.

As a final recommendation, we suggest more effort also be placed on Tl halide fiber technology to develop the low loss potential of these

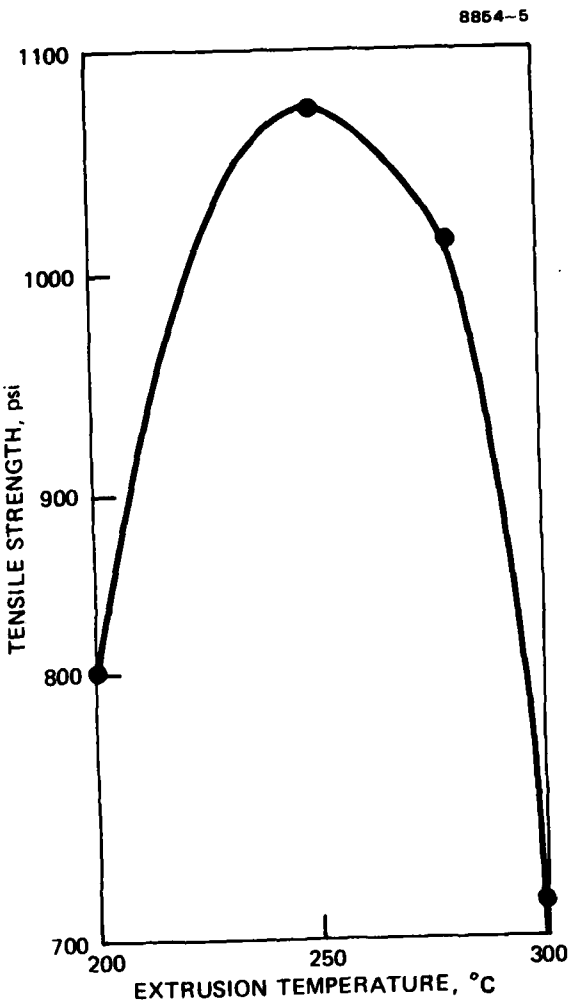

Figure 19.
Extruded KC1 fiber tensile yield strength versus extrusion temperature.

materials. To date, KRS-5 has been the best fiber at 10 μm, and, because of its extremely favorable physical properties (ductility, low melting point, etc.), it remains an excellent IR fiber candidate. The next step is to pruify it (by RAP chemistry) to further improve the fiber's transmission. In addition, KRS-5 is also a good choice for hot-rolling and single-crystal fiber growth.

E. DELIVERIES

The original contract plan called for periodic deliveries of fiber. After an initial delivery (6 months after the start of the contract) of KCl fibers, we observed the poor surface quality problems developing with KCl and, therefore, decided to postpone future deliveries until better fiber could be made. At the end of the contract, we still have not been able to improve the KCl fiber and thus we have decided to deliver the following fiber to meet the program requirements:

- The best KCl fiber fabricated: 8 m of 500-μm-diameter KCl fiber with a Parafilm M lubricant.
- The best IR fiber to date: 20 m of 250-μm-diameter KRS-5 fiber.

SECTION 3

PAPERS AND PRESENTATIONS

1. A.L. Gentile, M. Braunstein, D.A. Pinnow, J.A. Harrington, D.M. Henderson, L.M. Hobrock, J. Myer, R.C. Pastor, and R.R. Turk, "Infrared Fiber Optical Materials," in Fiber Optics: Advances in Research and Development, ed. by B. Bendow and S.S. Mitra, pp. 105-118, Plenum Publishing, N.Y., 1977.

2. J.A. Harrington. "Infrared Fiber Optics," Presented at 27th National IRIS, Materials Specialty Group, May 16, 1979, San Diego, CA.

3. J.A. Harrington. "Infrared Optical Fiber Waveguides," Presented at CLEOS "80," February 28, 1980, San Diego, CA.

4. J.A. Harrington, "Infrared Fiber Optics for CO_2 Laser Applications," in CO2 Laser Devices and Applications, Proceedings of SPIE Technical Symposium East, Vol. 227, Fall, 1980. Presentation at SPIE Meeting, April 11, 1980, Washington, D.C.

5. J.A. Harrington, M. Braunstein, B. Bobbs, and R. Braunstein, "Scattering Losses in Single and Polycrystalline Materials for Infrared Fiber Applications." Presented at Physics of Fiber Optics, American Ceramic Society Meeting, April 28, 1980, Chicago, Illinois. To be published in the proceedings.

REFERENCES

1. S.D. Allen and J.A. Harrington, "Optical Absorption in KCl and NaCl at Infrared Laser Wavelengths," Appl. Opt., Vol. 17, pp. 1679-1680, 1978.

2. D.A. Pinnow, A.L. Gentile, A.G. Standlee, A.J. Timper, and L.M. Hobrock, "Polycrystalline Fiber Optical Waveguides for Infrared Transmission," Appl. Phys. Lett., Vol. 33, pp. 28-29, 1978.

3. A.L. Gentile, M. Braunstein, D.A. Pinnow, J.A. Harrington, D.M. Henderson, L.M. Hobrock, J. Myer, R.C. Pastor, and R.R. Turk, "Infrared Fiber Optical Materials," in Fiber Optics: Advances in Research and Development, ed. by B. Bendow and S.S. Mitra, pp. 105-118, Plenum Publishing, N.Y., 1977.

4. J.A. Harrington, "Infrared Fiber Optics for CO_2 Laser Applications," in CO_2 Laser Devices and Applications, Proceedings of SPIE Technical Symposium East, Vol. 227, Fall, 1980.

5. L.G. Van Uitert and S.H. Wemple, "$ZnCl_2$ Glass: A Potential Ultralow-Loss Optical Fiber Material," Appl. Phys. Lett., Vol. 33, pp. 57-59, 1978.

6. M. Robinson, R.C. Pastor, R.R. Turk, D.P. Devor, M. Braunstein, and R. Braunstein. "Infrared-Transparent Glasses from the Fluorides of Zirconium, Thorium, and Barium," Mat. Res. Bull., to be published, 1980.

7. M. Poulain, M. Chanthanasinh, and J. Lucas, "New Fluoride Glasses," Mat. Res. Bull., Vol. 12, pp. 151-156, 1977.

8. D. Chen, R. Skogman, G.E. Bernal, and C. Butter, "Fabrication of Silver Halide Fibers by Extrusion," in Fiber Optics: Advances in Research and Development, ed. by B. Bendow and S.S. Mitra, pp. 119-122, Plenum Publishing, N.Y. 1977.

9. S. Kobayashi, N. Shibata, S. Shibata, and T. Izawa, "Characteristics of Optical Fibers in Infrared Wavelength Region," Rev. of Elect. Comm. Lab. (Japan), Vol. 26, pp. 453-468, 1978.

10. R.C. Pastor and A.C. Pastor, "Crystal Growth in a Reactive Atmosphere," Mat. Res. Bull., Vol. 10, pp. 117-124, 1975.

APPENDIX A

SCATTERING LOSSES IN SINGLE AND POLYCRYSTALLINE MATERIALS FOR INFRARED FIBER APPLICATIONS

J.A. Harrington and M. Braunstein

Hughes Research Laboratories†

Malibu, CA 90265

B. Bobbs* and R. Braunstein

University of California at Los Angeles††

Los Angeles, CA 90024

ABSTRACT

Polycrystalline fiber waveguides, fabricated from infrared transparent solids such as KRS-5 and KCl, have measured losses much greater than conventional silica fibers. One major source of these losses is scattering from grain boundaries present in the polycrystalline fibers. To improve the optical transmission of our infrared waveguides, we have studied the losses due to scattering in single and polycrystalline materials which are suitable for fabrication into infrared transmissive waveguides.

*Hughes Staff Doctoral Fellow.

†This work has been supported by Hughes Aircraft Company internal research and development programs and by RADC, Hanscom AFB, Mass.

††This work has been supported in part by AFOSR and ARO (Durham).

INTRODUCTION

Optical fiber waveguides made from crystalline materials such as KRS-5 (TlBrI), TlBr, AgCl, and KCl have been used for a variety of 10.6-μm, CO_2 laser applications.[1-4] The losses in the current IR fibers, however, are high (lowest loss measured is 300 dB/km at 10.6 μm in KRS-5) and applications in sensor and laser power delivery systems have been limited to short (1- to 2-m) lengths of fiber.[2-4] This measured IR fiber attenuation is considerably higher than that predicted theoretically for these and related IR transparent materials.[2,5] In fact, Gentile et al.[2] and van Uitert and Wemple[5] have shown that these materials have projected losses as low as 10^{-3} dB/km near 5 μm. To develop this ultra-low-loss potential, for such applications as long-distance communication links, requires a careful analysis of the nature of the attenuation mechanisms present in IR transparent waveguides. In this paper, we address the contribution of scattering to the total attenuation in bulk materials that have the potential for being fabricated into highly transparent fibers.

The attenuation mechanisms present in low-loss solids are illustrated in Fig. 1 for fused silica. At the shortest wavelengths, electronic processes (Urbach tail) contribute heavily to the total loss. At the IR wavelengths of interest, however, two mechanisms — scattering and multiphonon absorption — have been identified as the ultimate, limiting loss processes.[2] In Fig. 1, the curves for

scattering (which decreases as λ^{-4} with increasing wavelength) and lattice (multiphonon) absorption (which increases exponentially with increasing wavelength) cross to yield a minimum in the total attenuation. For fused silica, this minimum, which is about 0.25 dB/km at 1.6 μm, has been achieved in kilometer-long fibers.[6] For certain crystalline as well as special glassy solids, minima occur near 5 μm with projected losses well below the intrinsic losses measured in silica (projected losses are given in the next section).

The total attenuation coefficient α_T may be written as the sum

$$\alpha_T = \alpha_S + \alpha_A \quad , \tag{1}$$

where α_S and α_A are the contributions due to scattering and absorption, respectively. Each term in Eq. 1 can be measured independently, thus allowing the individual mechanisms contributing to the overall optical loss in solids to be studied. For example, α_T can be obtained from standard spectroscopic and fiber insertion loss measurements while laser calorimetry has been used very successfully to determine residual absorption α_A in weakly absorbing materials. The scattering terms α_S has not been as well studied. Measurements using integrating spheres for both bulk and fiber materials are generally used to obtain a total integrated scattering (TIS) loss.

These methods, however, have the disadvantage of being unable to distinguish among the various individual scattering mechanisms contributing to TIS. To elucidate the various scattering mechanisms as well as to obtain a value for α_s, we have chosen to study the light scattering spectra of solids. These spectra are composed of elastically (Rayleigh) scattered light that results from various nonpropagating fluctuations in the materials index of refraction and inelastically (Brillouin) scattered light that results from the interaction of light and the thermal motion of ions (sound waves). Although Rayleigh-Brillouin (RB) spectra have been used to measure α_s in glasses,[7] this technique has not been expressly used before to study scattering losses in single- and poly-crystalline materials. In this work, we have measured RB scattering at 90° in bulk single- and poly-crystalline KCl. As discussed in the next section, we expect very little Rayleigh scattering in single-crystal materials; for polycrystalline samples, however, intuition suggests that the residual strain and grain boundaries associated with the hot press-forged, polycrystalline material should lead to larger amounts of scattering. Our preliminary results support this presumption, but we have not yet been able to account for the source of each scattering mechanism contributing to the RB spectra.

GENERAL CONSIDERATIONS

The limiting attenuation mechanisms in transparent solids are scattering and multiphonon absorption. These contributions have

been considered by several investigators in the context of projecting future ultra-low-loss materials for the next generation of fiber waveguides. Van Uitert and Wemple[5] have studied the potential of $ZnCl_2$ (a glass former) while Gentile et al.[2] and Pinnow et al.[1] have concentrated on the crystalline materials. In Fig. 2, we consider the projected transmission for KRS-5 and KCl and compare these predictions to fused silica. The curves in Fig. 2 show the characteristic V shape resulting from the crossing of the scattering (short wavelength) and multiphonon (long wavelength) attenuation mechanisms. The only scattering mechanism assumed in calculating the λ^{-4}-dependent scattering curve for KRS-5 and KCl was Brillouin scattering (α_B - see below). As mentioned above, the V-shaped curve for silica has essentially been traced out experimentally and thus silica fiber losses are now intrinsic. For KCl and KRS-5 (as well as for many other non-oxide ionic solids), however, Fig. 2 shows the extremely low loss potential for these materials near 5 μm.

To determine α_S from RB light scattering experiments requires a careful measurement of the intensity of both the Brillouin- and Rayleigh-scattered light. Brillouin scattering results from light that has been inelastically scattered (Bragg scattering) from acoustical phonons (sound waves). The frequency of the scattered light is Doppler shifted from the frequency of the laser light ω_L by an amount $\pm\Omega$:

$$\Omega = \frac{4\pi n V \sin(\theta/2)}{\lambda_o} \quad ,$$

where n is the index of refraction of the medium, v is the velocity of sound, θ is the scattering angle, and λ_o is the vacuum wavelength of the light. This frequency shift has been well studied in alkali halides.[8] The Rayleigh-scattered light (central maximum at ω_L) is due to scattering of light from nonpropagating fluctuations in the dielectric constant. In glasses, mechanisms which give rise to these fluctuations include: density variations resulting from the frozen-in, random variations in dielectric constant inherent in a disordered solid; concentration fluctuations resulting from the local compositional variations present in mixtures; and entropy fluctuations resulting from temperature variations.[7] Of the three, only entropy fluctuations, which are very weak, would be present in an ideal single crystal.

To obtain α_S, we first evaluate the intensity ratio of the Rayleigh (I_R) to the total Brillouin ($2I_B$) scattered light. This ratio is called, based on its use in light scattering in liquids, the Landau-Placzek ratio R_{LP} and is defined[7] as

$$R_{LP} \equiv \frac{I_R}{2I_B} \quad . \tag{2}$$

Strictly speaking, since I_R and thus R_{LP} are related to specific scattering mechanisms (such as those discussed above for glasses),

measured values of R_{LP} are generally regarded as a property of a given material (e.g., fused SiO_2 has an $R_{LP} \simeq 23$, while $33K_2O\text{-}67SiO_2$ has an $R_{LP} \simeq 10$).[9] In our experiments, we measure I_R without, in general, knowing the specific mechanisms contributing to the Rayleigh component of scattered light. Therefore, we should more appropriately speak of an effective Landau-Placzek ratio with I_R representing the intensity of the central maximum.

The measured R_{LP} is then used to calculate α_S, as described by Pinnow et al.[10] and others,[7,9] from the relationship

$$\alpha_S = \alpha_B(R_{LP} + 1) \quad , \tag{3}$$

where α_B, is the small residual attenuation coefficient due to Brillouin scattering alone. It is given by

$$\alpha_B = \frac{8\pi^3}{3} \frac{1}{\lambda_o^4} (n^8 P_{12}^2)\, k_B\, T B_T \quad , \tag{4}$$

where P_{12} is the photoelastic (Pockels) coefficient, T is the temperature, k_B is Boltzmann's constant, and B_T is the isothermal compressibility. For ideal single crystals, $I_R \simeq 0$, thus $R_{LP} \simeq 0$ and (from Eq. 3) $\alpha_S \simeq \alpha_B$. This leads to the scattering curves in Fig. 2 for KRS-5 and KCl, which were calculated from Eq. 4 alone, while the scattering for fused silica was calculated from Eq. 3 using $R_{LP} = 23$.

An interesting feature of measured R_{LP}s for crystalline solids is their dependence on polarization. For our single-crystal measurements in KCl, a [100] crystal orientation was used for most samples studies. With incoming light along the [100] direction and scattered light along the [010], the polarization of the incident and analyzed scattered light was either vertical (V) or horizontal (H) with respect to the scattering plane. For this geometry, we may determine the intensities of the Brillouin components from the selection rules for the rock salt structure (O_h) and the differential cross section.[11] The intensities I and allowed vibrational modes for the various polarizations (phonon momentum q along [110] direction) are summarized in the matrix given in Table 1a. Using the known photoelastic (P_{12} and P_{44}) and elastic (C_{11}, C_{12}, and C_{44}) constants for KCl,[12] we calculate the matrix elements in Table 1a and give them, normalized to I_{HH} (the weakest intensity), in Table 1b. Table 1b shows that the intensities of the longitudinal modes (frequency equal to 15.8 GHz) in VV polarization are much stronger than those in the other polarizations (transverse mode frequency equal to 7.2 GHz). This means that measured Landau-Placzek ratios may vary greatly depending on crystal orientation and polarization, with the smallest R_{LP} occurring for the VV polarization.

LIGHT SCATTERING MEASUREMENTS

The RB spectra were recorded using as a source an Ar-ion laser (Spectra Physics Model 165) delivering 10 to 300 mW of single-line power and a PZT-scanned Fabry-Perot spectrometer. The experimental set-up is shown in the block diagram in Fig. 3. The spectrometer is a Burleigh Instruments, Inc., actively stabilized Fabry-Perot interferometer with its associated photon counting electronics. Data acquisition is provided by a 512-channel Tracor-Northern multichannel analyzer (MCA). This MCA has proven essential for obtaining good S/N ratios for these crystals (between 2000 and 20,000 scans are generally accumulated for each spectrum).

To improve the contrast of the spectrometer, we added a three-pass attachment to the interferometer. This allowed us to readily detect the Brillouin components in the polycrystalline materials where the Rayleigh scattering is more intense. Fig. 4 shows the results of a 90° scattering measurement on polycrystalline KCl doped with 1.75% RbCl taken with the light passing once (one-pass) or thrice (three-pass) through the interferometer. The improved contrast in the three-pass case is obvious. Note in particular the resolution of the transverse modes in the three-pass case that has been lost in the Rayleigh wing in the one-pass case. Clearly, the three-pass arrangement, which has been used in all our measured data, is necessary to obtain a reliable R_{LP}. The resolution of the triple-pass Fabry-Perot spectrometer was 0.03 cm^{-1} (finesse equal to 50).

RESULTS OF LIGHT SCATTERING EXPERIMENTS

Measurements of scattering losses were made at 488.0 nm in bulk single and polycrystalline KCl. The KCl was reactive atmosphere process (RAP) single-crystal material[13] which was either used in oriented single-crystal (SC) or in hot-press forged, polycrystalline (P) form. The RB scattering data shown in Fig. 5 are for pure, single-crystal KCl oriented as shown in the insert. From the data, we can see the intense stokes (S) and anti-stokes (AS) longitudinal Brillouin components in the VV polarization. The Brillouin components are also seen to become weaker in VH (or HV) and HH polarization, which is in qualitative agreement with the results stated in Table 1 for this scattering geometry. Similar results were obtained for other RAP-grown KCl (SC) although the R_{LP}s were found to vary somewhat from sample to sample.

The data for polycrystalline KCl (average grain size, 10 μm) are shown for two polarizations in Fig. 6. We can see from these data the intense Rayleigh scattering typical of our polycrystalline samples. In this sample, we also note the presence of only longitudinal modes in VV polarization and transverse modes in VH polarization. This leads us to conclude that we have, by chance, illuminated an axis of high symmetry in this sample. Specifically, it would appear from the data that the crystallites are oriented along the [100] direction for this particular experiment. In general, we would expect to observe an admixture of L and T modes

consistent with a random orientation of polycrystalline samples.

Effective Landau-Placzek ratios have been calculated for these two samples from the data in Figs. 5 and 6. These data are summarized in Table 2. For the single-crystal KCl, R_{LP} is lowest for the VV polarization, as discussed above, but the R_{LP}s for other polarizations do not scale with the predicted Brillouin intensities (see Table 1). This is due to the polarization dependence of the Rayleigh-scattered light. Our measurements of I_R indicate that the Rayleigh scattered light is, as expected, most intense for the VV polarization. For this polarization, I_R is approximately 8 to 10 times stronger than when measured under HV, VH, or HH conditions. More detailed studies of the depolarization ratio might give insight into the nature of the static defect contribution to elastic scattering. In general, the values for R_{LP} obtained for polycrystalline KCl(P) are higher than those for KCl(SC) (see Table 2). Again, the VV polarization for this unoriented poly sample yields the lowest R_{LP} and the HH case yields the highest R_{LP} (this trend was also seen in another KCl(P) sample).

Table 2 also gives the values of α_S calculated from Eqs. 3 and 4, which, for KCl at 488.0 nm, reduce to,

$$\alpha_S = 1.5 \times 10^{-6} \, (R_{LP} + 1) \, cm^{-1} \quad .$$

These attenuation coefficients due to scattering may be compared to the absorption coefficients obtained for KCl by laser calorimetric measurements at 488.0 nm by Harrington et al.[14] They found $\alpha_A \cong 3 \times 10^{-4}$ cm^{-1} for KCl(P) and $\alpha_A < 2 \times 10^{-5}$ cm^{-1} for KCl(SC). We see, therefore, that the total attenuation $\alpha_T (= \alpha_A + \alpha_S)$ is largely due to scattering.

The nature of the Rayleigh scattering in our crystalline samples is not completely understood. The results indicate substantial elastic scattering beyond that predicted above theoretically from entropy fluctuations. One may consider this excess parasitic scattering as arising from mechanical and chemical defects in the crystal. Although all the KCl has been RAP purified, we cannot rule out different amounts of chemical impurities in each sample. It is also evident that residual strain is present in both single and polycrystalline samples (observed as birefringence in crossed polarizers). This strain, which one would intuitively expect to be greater in the hot-forged polycrystalline materials, can lead to substantial elastic scattering. In particular, one would suspect grain boundaries as a potentially strong source of Rayleigh scattering because impurities, voids, and high strain would be more prevalent in these areas.

In our polycrystalline samples, it was not possible to examine the scattering from a single grain boundary because the average grain size (10 μm) was much smaller than the scattering volume

(cylindrical volume, 350 μm long by 30 μm in diameter). Brody et al.,[15] however, were able to study elastic scattering from a single grain boundary in polycrystalline calcium fluoride (Irtran-3). In their measurements, the grain size (150 μm) was larger than the scattering volume and they found essentially no difference in the intensity of light scattered from within a crystallite to that scattered from a volume containing a grain boundary. One might conclude from their results that grain boundaries do not contribute to elastic scattering; however, to assess the effect of grain boundaries properly, one must study high-purity material with a low Rayleigh background. Our future experiments will look more closely at the effect as well as the importance of residual strain on the Rayleigh scattered light.

SUMMARY

Our RB scattering studies on bulk KCl have been an initial attempt to probe the mechanisms responsible for scattering losses in highly transparent materials. We have found that polycrystalline materials scatter more strongly than do single-crystal materials, but we have not as yet been able to explicitly associate a particular elastic scattering process with a finite contribution to the total scattering. Our results, however, do indicate that, even in these very pure KCl samples, there is more scattering than predicted for the ideal KCl crystals and thus future fiber waveguides from these low-loss materials may be limited

more by scattering than absorption losses. Consequently, it is important to study scattering in poly- and single-crystal materials to understand the origin of the Rayleigh scattering and thereby to determine methods of minimizing this contribution to the attenuation.

REFERENCES

1. D.A. Pinnow, A.L. Gentile, A.G. Standlee, A.J. Timper, and L.M. Hobrock, "Polycrystalline Fiber Optical Waveguides for Infrared Transmission," Appl. Phys. Lett., Vol. 33, pp. 28-29, 1978.
2. A.L. Gentile, M. Braunstein, D.A. Pinnow, J.A. Harrington, D.M. Henderson, L.M. Hobrock, J. Myer, R.C. Pastor, and R.R. Turk, "Infrared Fiber Optical Materials," in Fiber Optics: Advances in Research and Development, ed. by B. Bendow and S.S. Mitra, pp. 105-118, Plenum Publishing, N.Y., 1977.
3. D. Chen, R. Skogman, G.E. Bernal, and C. Butter, "Fabrication of Silver Halide Fibers by Extrusion," ibid, pp. 119-122.
4. J.A. Harrington, "Infrared Fiber Optics for CO_2 Laser Applications," in CO_2 Laser Devices and Applications, Proceedings of SPIE Technical Symposium East, Vol. 227, Fall, 1980.
5. L.G. Van Uitert and S.H. Wemple, "$ZnCl_2$ Glass: A Potential Ultralow-Loss Optical Fiber Material," Appl. Phys. Lett., Vol. 33, pp. 57-59, 1978.

6. S. Kobayashi, N. Shibata, S. Shibata, and T. Izawa, "Characteristics of Optical Fibers in Infrared Wavelength Region," Rev. of Elect. Comm. Lab. (Japan), Vol. 26, pp. 453-468, 1978.

7. For a review see J. Schroeder, "Light Scattering of Glass," in Treatise on Materials Science and Technology, Vol. 12 Glass 1: Interaction With Electromagnetic Radiation, pp. 157-222, Academic Press, 1977.

8. G.B. Benedek and K. Fritsch, "Brillouin Scattering in Cubic Crystals," Phys. Rev., Vol. 149, pp. 647-662, 1966.

9. J. Schroeder, R. Mohr, P.B. Macedo, and C.J. Montrose, "Rayleigh and Brillouin Scattering in K_2O-SiO_2 Glasses," J. Amer. Cer. Soc., Vol. 56, pp. 510-514, 1973.

10. T.C. Rich and D.A. Pinnow, "Total Optical Attenuation in Bulk Fused Silica," Appl. Phys. Lett., Vol. 20, pp. 264-266, 1972.

11. W. Hayes and R. Loudon, "Scattering of Light by Crystals, pp. 327-353, J. Wiley & Sons, 1978.

12. Landolt-Bornstein Numerical Data and Functional Relationships in Science and Technology, New Series, ed. by K.H. Hellwege and A.M. Hellwege, Vol. II, pp. 25, 29, 510, and 513, Springer-Verlag, 1979.

13. R.C. Pastor and A.C. Pastor, "Crystal Growth in a Reactive Atmosphere," Mat. Res. Bull., Vol. 10, pp. 117-124, 1975.

14. J.A. Harrington, B.L. Bobbs, M. Braunstein, R. Kim, R. Stearns, and R. Braunstein, "Ultraviolet-Visible Absorption in Highly Transparent Solids by Laser Calorimetry and Wavelength Modulation Spectroscopy," Appl. Opt., Vol. 17, pp. 1541-1546, 1978.

15. E. Brody, C. Roychoudhuri, and M. Hercher, "Brillouin Spectra of CaF_2 Microcrystals Using a Stable 3-Pass Fabry-Perot Interferometer," Appl. Phys. Lett., Vol. 23, pp. 543-545, 1973.

TABLE I

Intensities of Brillouin Components for a Rocksalt Crystal

(a)

Mode	I_{VV}	$I_{VH} = I_{HV}$	I_{HH}
(110) L	$\frac{4P_{12}^2}{C_{11} + C_{12} + C_{44}}$	0	$\frac{4P_{44}^2}{C_{11} + C_{12} + C_{44}}$
(1$\bar{1}$0) T	0	0	0
(001) T	0	$\frac{P_{44}^2}{2C_{44}}$	0

(b)

Mode	I_{VV}	I_{VH}	I_{HH}
(110) L	133	0	1
(1$\bar{1}$0) T	0	0	0
(001) T	0	4.8	0

TABLE II

Effective R_{LP} and Calculated Values of α_S

Structure	Polarization	R_{LP}	α_S (cm^{-1})
Single	VV	26.2	4.1×10^{-5}
Crystal	VH	38.5	5.9×10^{-5}
(SC)	HV	44.9	6.9×10^{-5}
	HH	276.4	4.2×10^{-4}
Polycrystalline	VV	496	7.5×10^{-4}
(P)	VH	830	1.2×10^{-3}
	HV	1598	2.4×10^{-3}
	HH	>5000	$>7.5 \times 10^{-3}$

FIGURE CAPTIONS

Fig. 1 - Schematic representation of optical attenuation mechanisms in solids.

Fig. 2 - Projected losses for some IR transparent materials. Short wavelengths are bounded by $1/\lambda^4$-scattering and long wavelengths by multiphonon absorption.

Fig. 3 - Block diagram of scanning Fabry-Perot interferometer for measuring RB spectra.

Fig. 4 - Improved contrast in RB spectra of poly KCl + 1.75% RbCl through the use of 3-pass attachment on Fabry-Perot interferometer. The spectra were all recorded using the 3-pass configuration.

Fig. 5 - Scattering spectra for single-crystal KCl for three different polarizations. Landau-Placzek ratios are given in Table 2 for these data.

Fig. 6 - Scattering spectra for polycrystalline KCl (average grain size is 10 μm). Landau-Placzek ratios are given in Table 2 for these data.

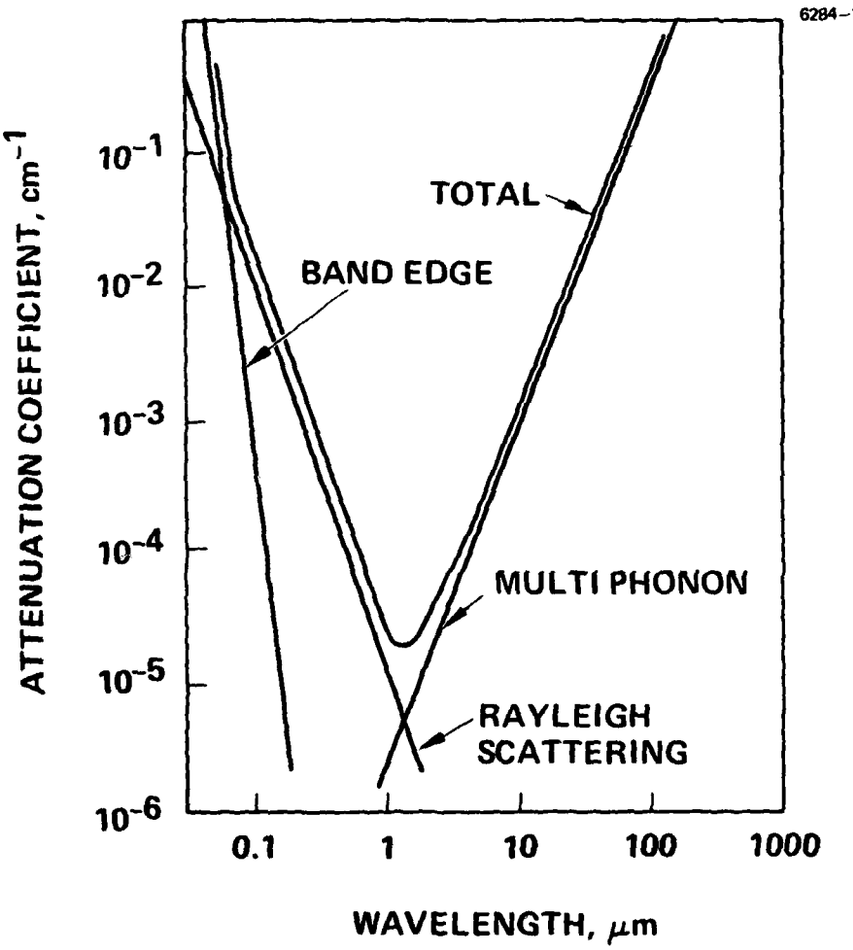
6284-1
ATTENUATION COEFFICIENT, cm^{-1}
10^{-1}
10^{-2}
10^{-3}
10^{-4}
10^{-5}
10^{-6}
TOTAL
BAND EDGE
MULTI PHONON
RAYLEIGH SCATTERING
0.1
1
10
100
1000
WAVELENGTH, μm

Figure 1.

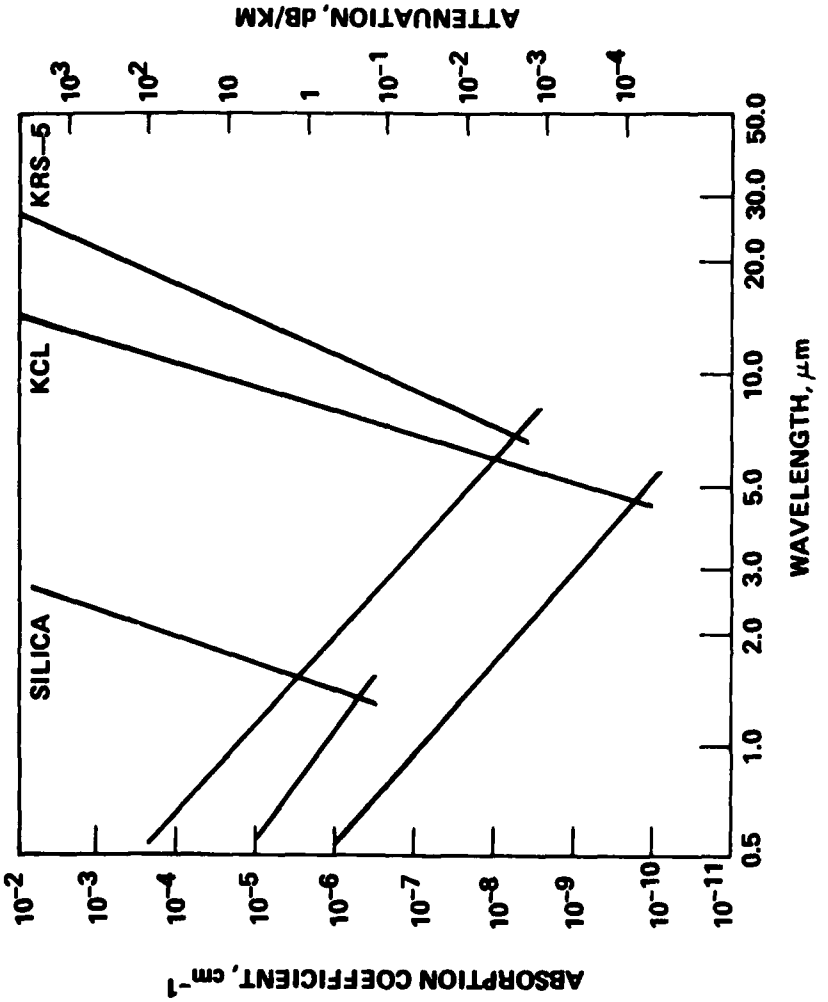
9467-1
ATTENUATION, dB/KM
10^{3}
10^{2}
10
1
10^{-1}
10^{-2}
10^{-3}
10^{-4}
KRS–5
KCL
SILICA
0.5
1.0
2.0
3.0
5.0
10.0
20.0
30.0
50.0
WAVELENGTH, μm
10^{-2}
10^{-3}
10^{-4}
10^{-5}
10^{-6}
10^{-7}
10^{-8}
10^{-9}
10^{-10}
10^{-11}
ABSORPTION COEFFICIENT, cm^{-1}

Figure 2.

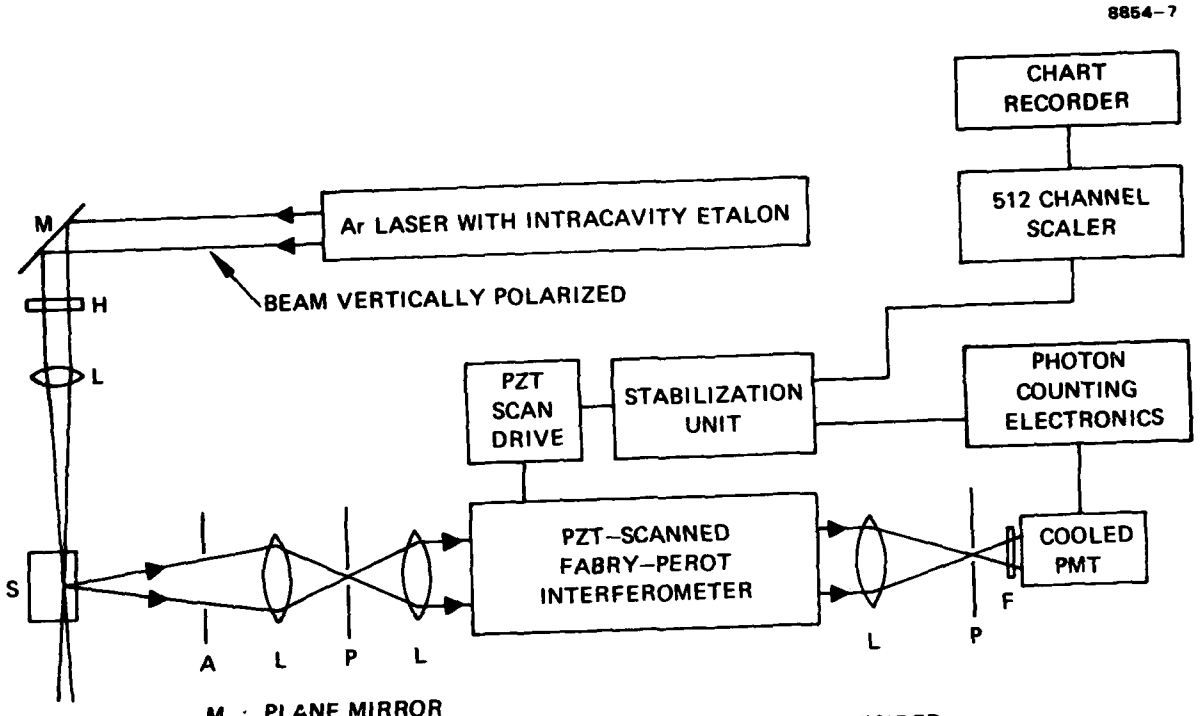

M : PLANE MIRROR
H : HALFWAVE PLATE TO ROTATE POLARIZATION IF DESIRED
L : LENSES TO FOCUS AND COLLIMATE LIGHT
S : TRANSPARENT SAMPLE
A : APERTURE TO LIMIT RANGE OF SCATTERING ANGLES DETECTED
P : PINHOLES TO BLOCK OFF-AXIS LIGHT
F : NARROWBAND (30 Å) FILTER TO BLOCK FLUORESCENCE, RAMAN SCATTERING AND BACKGROUND RADIATION

Figure 3.

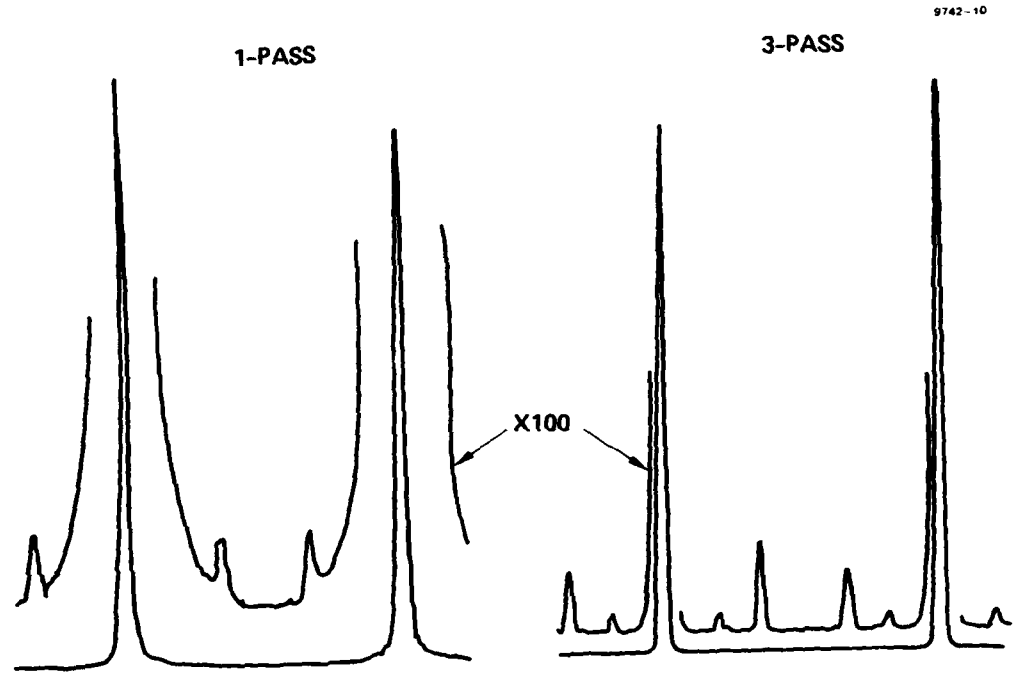

Figure 4.

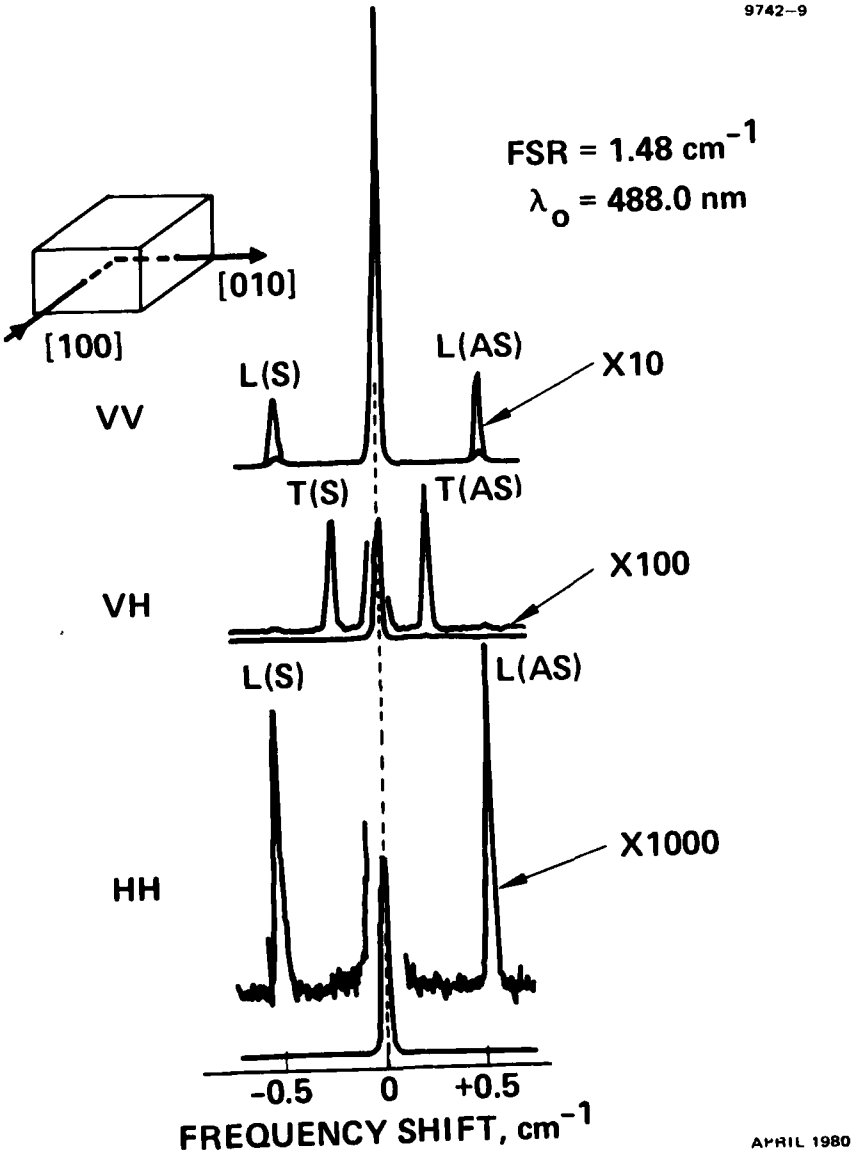
9742-9
FSR = 1.48 cm^{-1}
λ_o = 488.0 nm
[010]
[100]
L(S)
L(AS)
X10
VV
T(S)
T(AS)
X100
VH
L(S)
L(AS)
X1000
HH
-0.5
0
+0.5
FREQUENCY SHIFT, cm^{-1}
APRIL 1980

Figure 5.

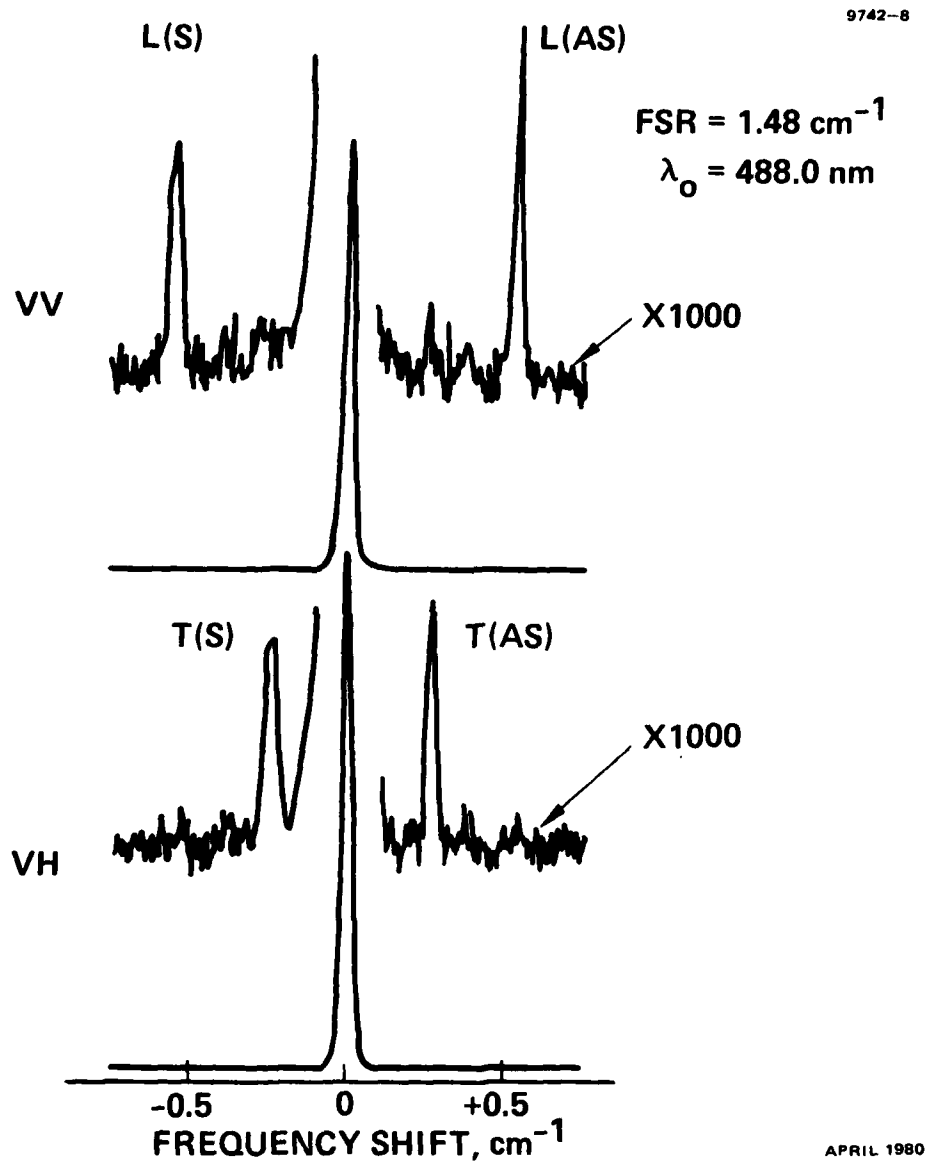
9742-8
L(S)
L(AS)
FSR = 1.48 cm^{-1}
λ_o = 488.0 nm
VV
X1000
T(S)
T(AS)
X1000
VH
-0.5
0
+0.5
FREQUENCY SHIFT, cm^{-1}
APRIL 1980

Figure 6.

APPENDIX B

Presented at SPIE Meeting, Washington, D.C., April 1980

Infrared fiber optics for CO_2 laser applications

James A. Harrington

Hughes Research Laboratories
3011 Malibu Canyon Road, Malibu, California 90265

Abstract

Advances in the technology of fabricating IR transmissive fiber waveguides have resulted in the development of fibers that offer unique solutions to near- and long-term IR systems problems. Short (~2 m) links of polycrystalline KRS-5 (thallium bromoiodide) fiber have already been successfully used to relay information to remote photodetectors. Future long-distance communications links may take advantage of the extremely low loss potential ($\sim 10^{-3}$ dB/km) predicted theoretically for a large class of IR fiber materials near 5 μm.

Introduction

Conventional (glass) fiber-optic waveguides have been successfully used in a variety of communications and military systems. Certain sensor and communications systems, however, require fiber waveguides that operate at wavelengths longer than 2 μm — the approximate cutoff of silica fibers. To meet present and future demands for highly transmitting IR fiber optics, we have fabricated IR fibers from alkali and thallium halides, which transmit IR wavelengths up to 25 μm. These materials used for fiber waveguides offer solutions to several IR systems problems, including (1) the dissection of images in the focal plane for enhanced detection and signal processing with focal plane arrays, (2) the relay of focal planes to remote photodetectors, (3) flexible transmission of high-power CO and CO_2 laser beams for heating and machining in remote or inaccessible locations, and (4) extremely low-loss guided communications links. We have developed KRS-5 (thallium bromoiodide) fibers that are suitable for the first three applications. Additional work in waveguide design and material purification will be required before fibers are usable for ultra-low-loss communications links. The potential for such links using halide fibers operating near 5 μm is very great since their losses are theoretically predicted to be near 10^{-3} dB/km, or a factor of 1000 better than the best glass (silica) fibers at 1.6 μm. The achievement of IR fibers with these losses would greatly affect numerous communications systems that require kilometer-long, repeaterless fiber links.

Optical Properties of IR Fibers

There are many highly transmissive IR materials,[1] but only a few have been fabricated into IR fiber waveguides. The ductile thallium[2,3] and silver[4] halides have been successfully extruded into IR fibers with fiber diameters ranging from 75 to 1000 μm. Other halides such as KCl[3] and CsI have also been extruded, but with much poorer optical quality than, for example, our best KRS-5 fiber (300 dB/km). In this paper, our emphasis will be on KRS-5 fiber since this fiber has proven to be the best fiber for CO_2 laser applications.

The transparency of IR materials is limited by extrinsic and intrinsic loss mechanisms. The ultimate limiting loss mechanisms in solids are multiphonon absorption[1] at long wavelengths and scattering and electronic absorptions at the shorter wavelengths. Since, at the IR wavelengths of interest (2 to 10 μm), the electronic band edge (Urbach tail) is generally a very small contributor to total attenuation,[3] the scattering and multiphonon contributions combine to give the net intrinsic loss. These losses are shown in Figure 1 for fused silica,[5] KCl,[3] and KRS-5. Each material shows a characteristic V-shape curve composed of a λ^{-4}-type scattering loss (Rayleigh/Brillouin scattering) and an exponential multiphonon tail.[1] The minimum attenuation in silica is near 1.4 μm (~0.3 dB/km), and these losses have in fact been achieved in both bulk materials and fibers[6] (i.e., the V-curve for silica has been experimentally verified). The intrinsic losses for KCl and KRS-5 are seen from Figure 1 to be considerably less than for fused silica. For these crystalline materials, as well as for other alkali halides,[3,7] TlBr,[2,3] and $ZnCl_2$ glass,[7] the minima in the V-curve is generally 1000 times less than for silica. Unlike silica, however, the measured losses in both bulk crystalline materials and fibers in these hosts is well above the intrinsic limits embodied in these V-curves. For example, the lowest-loss bulk IR material measured to date is KCl[8] (absorption coefficient $\beta = 10^{-6}$ cm^{-1} = 0.4 dB/km at 5 μm), which is still three orders of magnitude above the intrinsic limit.

IR transmissive materials have not realized this potential for ultralow loss because extrinsic absorption mechanisms (e.g., impurity, mechanical defect, and surface absorption) dominate the total attenuation. These mechanisms are important in bulk IR materials.[9] In our polycrystalline fibers, additional mechanisms (e.g., scattering from grain boundaries and irregularities in the surface of the fiber) are expected to strongly increase fiber losses. Therefore, a major task is the elimination of extrinsic sources of absorption, by, for example, using purer materials and better fiber fabrication techniques.

We have extruded polycrystalline KCl, TlBr, KRS-5, and CsI fiber using a specially built extrusion press. Extrusion temperatures were in the range of 200 to 350°C for the thallium halides and 25 to 740°C for the alkali halides. Table 1 gives the measured absorption coefficients for the extruded fibers at 10.6 μm and, for comparison, the values of the calorimetrically[8,9,10] measured loss in the bulk material (note that fiber losses are given in dB/m since this unit more accurately represents the lengths of fiber actually measured

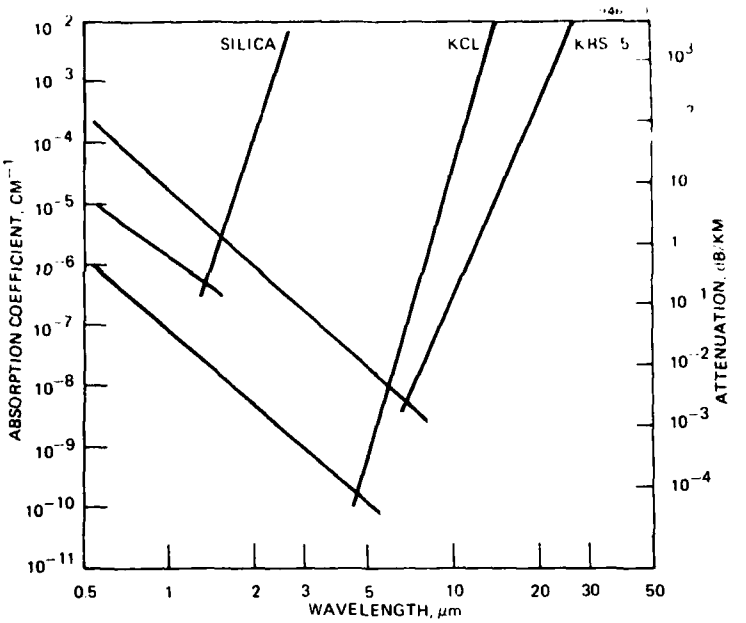

Figure 1. Intrinsic absorption limits in transparent materials. Short wavelength absorption is due to scattering while the long wavelength absorption is due to multiphonon process.

from 0.5 to 1.5 m). With its internal loss of ~7% per meter, KRS-5 is the best fiber material of the group. Another representation of this loss is given in Figure 2 for a 250-μm-diameter KRS-5 fiber. This fiber has an internal loss of 0.57 dB/m (external Fresnel loss for KRS-5 is 1.45 dB); extrapolating the data back to the ordinate[10] indicates that there is very little surface absorption. Extruded 500-μm-diameter KCl fiber has much higher losses because its very poor surface quality (fish-scale appearance) results in much of the light being scattered at the surface. Attempts to extrude KCl with a lubricant to reduce friction between the extrusion die and the fiber have not greatly improved the optical quality of the fiber. Results similar to those for KCl have also been obtained for CsI.

Table 1. Bulk Material and Fiber Losses at CO_2 Laser Wavelengths

Material	Absorption Coefficient at 10.6 μm, cm^{-1} (dB/m)	
	Bulk	Fiber
KRS-5	7×10^{-4} (0.3)	7×10^{-4} (0.3)
TlBr	1×10^{-3} (0.43)	1×10^{-3} (0.43)
KCl	8×10^{-5} (0.035)	1×10^{-2} (4.2)
KBr	1×10^{-5} (0.0004)	

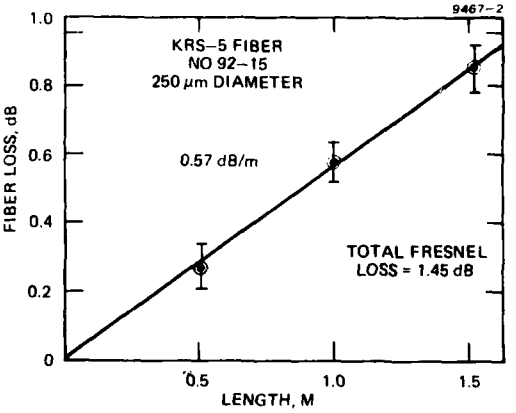

Figure 2. Bulk and surface absorption in KRS-5 fiber.

Measurement of the scattering losses in our fibers has been mostly qualitative. By placing liquid-crystal paper on top of a KRS-5 fiber as a means of visually inspecting the heating of a fiber irradiated with a CO_2 laser, we have found that the amount of heating observed is uniformly small over the entire length of the fiber in our best fibers. Older fibers of poorer optical quality have shown hot spots on the liquid-crystal paper or were uniformly very lossy. The hot spots can be removed and the transmission improved by cutting the fiber. Losses are also "visible" at points of sharp bends (~1-in. radius). When the fiber is straightened, the losses generally decrease unless the fiber has been permanently damaged (see the next section). More

quantitative experiments are underway to evaluate the scattering contribution independently by measuring the Rayleigh/Brillouin scattering spectrum of the single and polycrystalline fiber materials.[11]

The power-handling capability of KRS-5 fibers has been investigated using a CO_2 laser source. Figure 3 shows a 500-μm-diameter KRS-5 fiber delivering 2 W of CO_2 laser radiation.

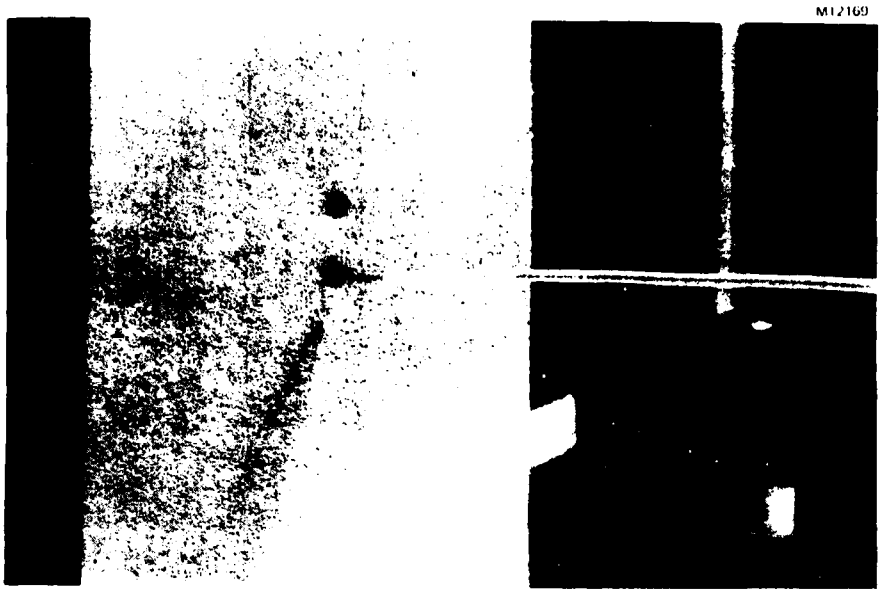

Figure 3. CO_2 laser power delivery by a 500-μm-diameter KRS-5 fiber.

The KRS-5 and TlBr fibers that we have been using for CO_2 laser applications are generally unclad. We have been unable to successfully clad the fiber using the conventional method for cladding silica fibers. Coextrusion, for example, of TlCl (n = 2.19) cladding on a KRS-5 (n = 2.37) core has produced a diffuse clad-core interface, caused by diffusion of TlCl into the KRS-5 core (along grain boundaries). This fiber had excessive losses. Similar results were obtained when post-cladding methods (such as for example) were tried. The best cladding we have found has been loose-fitting polyethylene tubing. This technique works well because there is minimal contact between the fiber and the tubing[3] and thus leakage is small.

Mechanical properties of IR fibers

The extruded fibers are polycrystalline with fiber grain sizes that range between 3 and 40 μm. The grain size is a function of the extrusion temperature: the higher the temperature, the larger the grain size. Figure 4 shows 100-μm-diameter KRS-5 fiber extruded at two different temperatures.

Fiber strength is a function of fiber grain size. Yield and ultimate strength are greatest for small grain size fiber, decreasing as grain size increases (see Figure 5). Good 10.6-μm transmission has been measured for both small and large grain fibers. But the stronger, small-grain-size fiber is more desirable for most CO_2 laser applications. Table 2 summarizes the mechanical properties of our 100-μm-diameter fiber.

The flexural properties of IR and glass (silica) fibers are, of course, quite different. TlBr fiber is very flexible at room temperature, as shown qualitatively in Figure 6. KRS-5 fiber (250-μm diameter) may be bent to a radius of 6 in. without degradation. Warming the fiber slightly above room temperature makes this fiber even more flexible.

Fiber failure occurs when grain boundaries separate. This may be seen in Figure 7 for KRS-5 fiber. The fiber in Figure 7(a) has been stretched, revealing the separated grain boundaries (note, fiber does not neck-down). A complete break (Figure 7(b)) occurs at grain boundaries, leaving a jagged fiber end.

Applications of IR fibers

The applications of IR fibers are most easily discussed in terms of laser power transmission or the communication of information. Power applications using CO_2 lasers rely on the delivery of relatively small amounts of power to remote or inaccessible locations. One such use would be in laser surgery, where a flexible fiber would deliver laser radiation for applications in dentistry, neurosurgery, ophthalmology, and urology. Another power application involves laser cutting and drilling. In this area, a fiber bundle could accept CO_2 laser

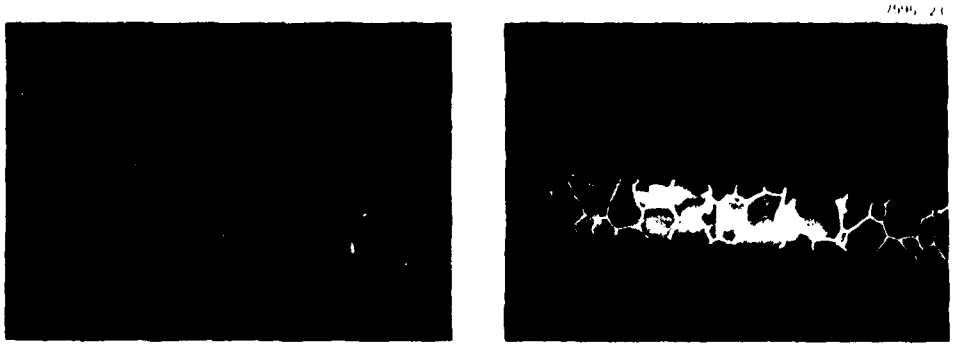

Figure 4. Fiber grain structure in 100-μm-diameter KRS-5 fiber.

Table 2. echanical Properties of IR Fibers

Tensile Tests[a]	KRS-5	TlBr
Ultimate strength, psi	9000 (6)[b]	3800 (4)
Yield strength, psi	5400 (9)	3200 (4)
Elongation,	3.1 (5)	1.2 (4)
Modulus of elasticity	1.8×10^6 (4)	0.8×10^6 (4)

[a]Tests made at 10 cm gauge length, 0.02 cm/min strain rate.

[b]Number of samples tested.

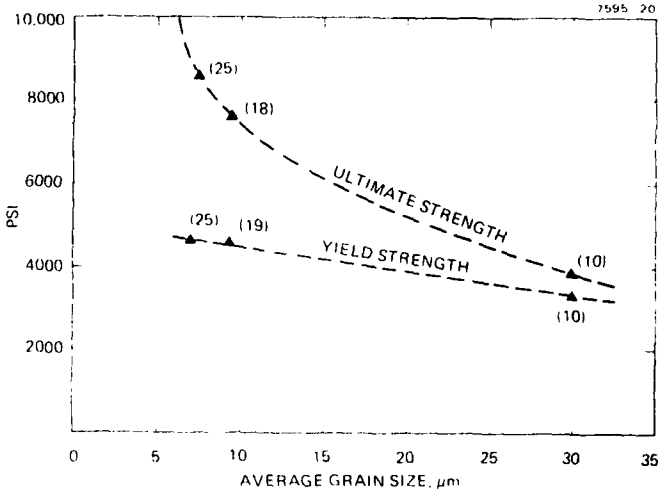

Figure 5. Strength of 100-μm-diameter KRS-5 fiber as a function of fiber grain size.

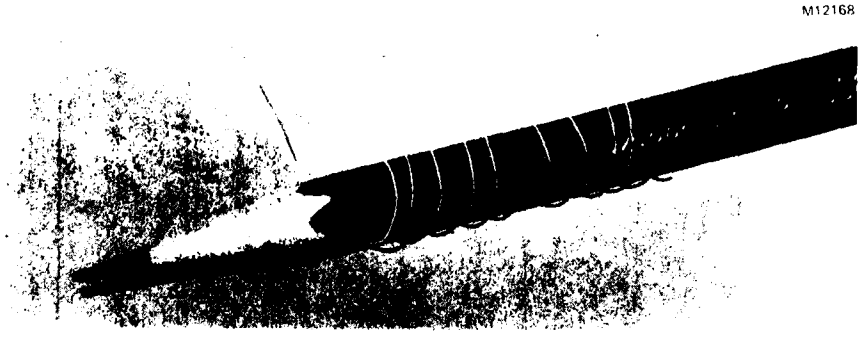

Figure 6. Coiled TlBr fiber to show flexural properties.

...tion and distribute power to remote locations. Potential uses include cloth cutting and multiple hole ...

...ow-loss potential of IR fibers (see Figure 1) has enormous importance to future communications ... tion of IR fiber with losses as low as 10^{-3} dB/km will allow long-distance communications sys- ... lt in which repeaters would not be needed. For example, an undersea (repeaterless) communica- ... of kilometers long is anticipated. Our work on KCl fiber is directed toward understanding ... and preparing ultra-low-loss IR fiber.

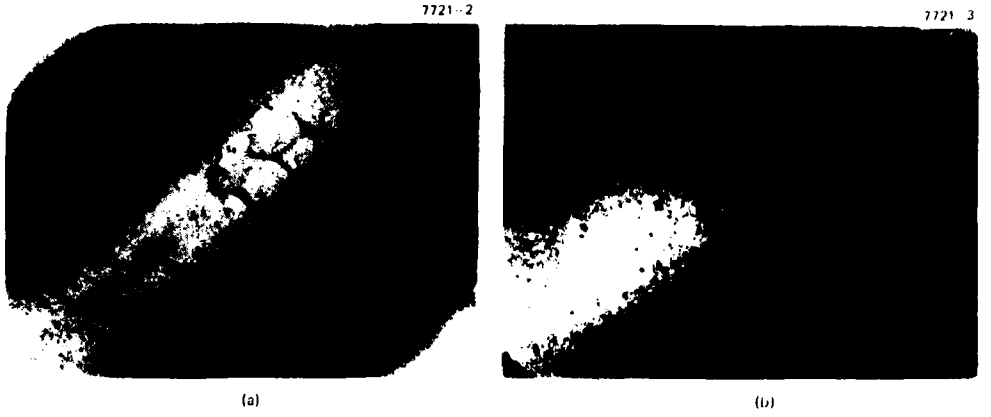

Figure 7. Mechanical failure of KRS-5 fiber.

Nearer-term applications necessarily involve shorter lengths of IR fiber (1 to 2 m). Defense systems may take advantage of the IR transparency of KRS-5 fiber (2 to 25 μm) to relay information from remote areas to photodetectors. In this application, the IR fiber would serve as a passive detector of IR radiation with the usual fiber advantages of immunity to electromagnetic interference (EMI) and resistance to jamming. We successfully tested this application by building an IR fiber receiver using two 250-μm-diameter KRS-5 fibers (each 60 cm long) to link the received signal (CO_2 laser pulses) to two cooled photodetectors. A similar application could be made in pyrometry. The long-wavelength blackbody radiation transmitted by KRS-5 fiber (near 10 μm) makes the measurement of low temperatures (less than 100°C) possible.

Conclusions

The art of fabricating IR transmissive waveguides has progressed to the point that many short-length (~10 m) applications are now possible. These applications include CO_2 laser power transmission and transmission of information at IR wavelengths. The effect on future communications systems will be great if the ultra-low-loss potential of these IR fiber materials can be realized.

Acknowledgments

The author wishes to thank D.H. Henderson, M. Braunstein, R.R. Turk, and T.A. Pinnow for helpful discussions and A. Standlee for fiber extrusion and optical measurements. This research has been supported in part by Hughes Aircraft Company IR&D programs.

References

1. Bendow, B., "Multiphonon Infrared Absorption in the Highly Transparent Frequency Regime of Solids," in Solid State Physics, ed. by Seitz and Turnbull, Academic Press, N.Y. Vol. 33, pp. 249-316, 1978.

2. Pinnow, D.A., Gentile, A.L., Standlee, A.G., Timper, A.J., and Hobrock, L.M., "Polycrystalline Fiber Optical Waveguides for Infrared Transmission," Appl. Phys. Lett., Vol. 33, pp. 28-29, 1978.

3. Gentile, A.L., Braunstein, M., Pinnow, D.A., Harrington, J.A., Henderson, D.M., Hobrock, L.M., Myer, J., Pastor, R.C., and Turk, R.R., "Infrared Fiber Optical Materials," in Fiber Optics: Advances in Research and Development, ed. by B. Bendow and S.S. Mitra, Plenum Publishing, N.Y., 1979. pp. 105-118.

4. Chen, D., Skogman, R., Bernal G, E., and Butter, C., "Fabrication of Silver Halide Fibers by Extrusion," ibid, pp. 119-122.

5. Pinnow, D.A., Rich, T.C., Ostermayer, Jr., F.W., DiDomenico, Jr., M., "Fundamental Optical Attenuation Limits in the Liquid and Glassy State with Application to Fiber Optical Waveguides," Appl. Phys. Lett., Vol. 22, pp. 527-529, 1973.

6. Kobayashi, S., Shibata, N., Shibata, S., and Izawa, T., "Characteristics of Optical Fibers in Infrared Wavelength Region," Rev. of Elect. Comm. Lab. (Japan), Vol. 26, pp. 453-468, 1978.

7. Van Uitert, L.G. and Wemple, S.H., "$ZnCl_2$ glass: A Potential Ultralow-loss Optical Fiber Material," Appl. Phys. Lett., Vol. 33, pp. 57-59, 1978.

8. Allen, S.D. and Harrington, J.A., "Optical Absorption in KCl and NaCl at Infrared Laser Wavelengths," Appl. Opt., Vol. 17, pp. 1679-1680, 1978.

9. Hass, M. and Bendow, B., "Residual Absorption in Infrared Materials," Appl. Opt., Vol. 16, pp. 2882-2890, 1977.

10. Rowe, J.M. and Harrington, J.A., "Temperature Dependence of Surface and Bulk Absorption in NaCl and KCl at 10.6 μm," Phys. Rev. B, Vol. 14, pp. 5442-5450, 1976.

11. Rich, T.C. and Pinnow, D.A., "Total Optical Attenuation in Bulk Fused Silica," Appl. Phys. Lett., Vol. 20, pp. 264-266, 1972.

MISSION
of
Rome Air Development Center

RADC plans and executes research, development, test and selected acquisition programs in support of Command, Control Communications and Intelligence (C^3I) activities. Technical and engineering support within areas of technical competence is provided to ESD Program Offices (POs) and other ESD elements. The principal technical mission areas are communications, electromagnetic guidance and control, surveillance of ground and aerospace objects, intelligence data collection and handling, information system technology, ionospheric propagation, solid state sciences, microwave physics and electronic reliability, maintainability and compatibility.

Printed by
United States Air Force
Hanscom AFB, Mass. 01731